

# Tropical Geometry of Phylogenetic Tree Space: A Statistical Perspective

Anthea Monod<sup>1,†</sup>, Bo Lin<sup>2</sup>, Ruriko Yoshida<sup>3</sup>, and Qiwen Kang<sup>4</sup>

1 Department of Mathematics, Imperial College London, UK

2 Department of Mathematics, University of Texas, Austin, TX, USA

3 Department of Operations Research, Naval Postgraduate School, Monterey, CA, USA

4 Medpace, Inc. and Department of Statistics, University of Kentucky, Lexington, KY, USA

† Corresponding e-mail: a.monod@imperial.ac.uk

## Abstract

Phylogenetic trees are the fundamental mathematical representation of evolutionary processes in biology. As data objects, they are characterized by the challenges associated with “big data,” as well as the complication that their discrete geometric structure results in a non-Euclidean phylogenetic tree space, which poses computational and statistical limitations. We propose and study a novel framework to study sets of phylogenetic trees based on tropical geometry. In particular, we focus on characterizing our framework for statistical analyses of evolutionary biological processes represented by phylogenetic trees. Our setting exhibits analytic, geometric, and topological properties that are desirable for theoretical studies in probability and statistics, as well as increased computational efficiency over the current state-of-the-art. We demonstrate our approach on seasonal influenza data.

**Keywords:** BHV tree space; phylogenetic tree space; tree metric; tropical geometry; tropical metric.

## 1 Introduction

Evolutionary relationships describing how organisms are related by a common ancestor are represented in a branching diagram known as a *phylogenetic tree*. Phylogenetic trees model many important and diverse biological phenomena, such as speciation, the spread of pathogens, and cancer evolution. Methodology to analyze phylogenetic datasets has been under active research for several decades for two important reasons. First, explicit computations directly on collections of phylogenetic trees are challenging due to extremely high dimensionality. Second, standard statistical methodologies are not directly applicable due to the non-Euclidean nature of the setting. Significant previous work addresses various classical statistical interests, however a fundamental breakthrough for quantitative studies on sets of trees emerged through studying the geometry of the set of all phylogenetic trees (Billera et al., 2001).

Referred to in the literature as *BHV tree space*, the set of all phylogenetic trees is constructed as a moduli space, where each phylogenetic tree is represented as an individual point. The geometry is characterized by a unique geodesic between any two points; its length defines a metric on the space. Since its introduction in 2001, it has been actively studied in various wide-reaching domains, including algebraic geometry, category theory, computational biology, and statistical genetics (e.g., Baez and Otter (2017); Devadoss and Morava (2015); Nye et al. (2017); Weyenberg and Yoshida (2016)). Despite its indisputable significance, the BHV geometry nevertheless poses important data-analytic complications for both descriptive and inferential statistics.

Considering an alternative approach based on *tropical geometry*—a variant of algebraic geometry—alleviates such complications. The first formal relation between tropical geometry and mathematical phylogenetics arises in a homeomorphism between the space of phylogenetic trees and a tropical algebraic variety (Speyer and Sturmfels, 2004). This coincidence has been further studied in theoretical research (e.g., Ardila and Klivans (2006); Manon (2011)), however, its implication and potential in applied work remain largely untapped.

In this paper, we harness the linearizing properties of the tropical geometric interpretation of phylogenetic tree space for quantitative and statistical analysis within the framework of metric geometry. Our approach is

characterized by an explicit *tropical metric*; we refer to the resulting metric space as *palm tree space* (tropical tree space). We show that mathematical properties of palm tree space provide the existence of fundamental statistical quantities—such as probability measures, means, and variances—ensuring that statistical and probabilistic studies are well defined, and more generally, are desirable for analytics and computation. Our framework lends a novel computational perspective to the set of all phylogenetic trees, which effectively results in a more natural setting for statistics: in the same way that linear algebra underlies classical statistics, the tropical metric allows for a tropical interpretation of linear algebra on non-Euclidean tree space.

The remainder of this paper is organized as follows. In Section 2, we provide detail on the mathematical setting for our contributions. Specifically, we give the relationship between phylogenetic trees and metrics in the context of tropical geometry; this section also provides a literature overview. In Section 3, we introduce and discuss formal properties of the tropical metric on the space of phylogenetic trees and formally define palm tree space. We study its geometry, topology, and analytic properties. We also give some examples of theoretical probability measures used in statistics and that are important in probability theory. In Section 4, we give an example of a statistical analysis on real data in the setting of palm tree space and compare its performance against the BHV standard. We close in Section 5 with a discussion, and some ideas for future research.

## 2 Tropical Geometry and Tree Metrics

In this section, we introduce the essentials of tropical geometry for our study, and we provide a review of occurrences of tropical geometry in data analytic and statistical settings. We also discuss the representation of phylogenetic trees as metrics and give some examples of important and commonly-occurring tree metrics used in applications.

### 2.1 Basics of Tropical Geometry

Tropical algebra is a branch of abstract algebra based on specific semirings, which we now define. The extension of tropical algebra to tropical geometry is a variant of algebraic geometry: in algebraic geometry, geometric properties of zero sets of systems of multivariate polynomials are studied; in tropical geometry, these polynomials are defined in the tropical algebra.

**Definition 1.** The *tropical (max-plus) semiring* is  $(\mathbb{R} \cup \{-\infty\}, \boxplus, \odot)$ , with addition and multiplication given respectively by

$$a \boxplus b := \max(a, b) \quad \text{and} \quad a \odot b := a + b.$$

*Remark 2.* In the literature on tropical geometry (e.g., Speyer and Sturmfels (2009)), the term “tropical” typically refers to min-plus addition (where addition is given by the minimum between two elements, rather than their maximum), denoted by  $\oplus$ , where the semiring is  $(\mathbb{R} \cup \{\infty\}, \oplus, \odot)$ , isomorphic to the max-plus semiring. As will be further discussed in the context of phylogenetic tree metrics, we adopt the max-plus convention for consistency.

Note that tropical subtraction is not defined in this semiring. *Tropicalization* means replacing the standard arithmetic operations with their tropical counterparts. Using these arithmetic operations, usual mathematical relations and objects of interest may be studied, such as lines, functions, and sets. Tropicalized mathematical objects are piecewise linear constructions due to the linearizing binary operations on the tropical semiring. For example, the tropically quadratic polynomial  $x^2 \boxplus 1$  is given by  $x \odot x \boxplus 1 = \max(2x, 1)$  in standard arithmetic. These linearizing properties are desirable for increased computational efficiency. See Maclagan and Sturmfels (2015) for a formal treatment of tropical geometry in full detail with examples.

### 2.2 Phylogenetic Trees and Metrics

A *phylogenetic tree* is an acyclic connected graph,  $T = (V, E)$ , where  $V$  is the set of labeled terminal nodes called *leaves* with degree 1, and  $E$  is the set of *edges* or *branches*, each with positive length representing evolutionary time. Non-leaf vertices in a phylogenetic tree have degree at least 2. Edges connecting to leaves are called *external edges*; otherwise, they are *internal edges*. Phylogenetic trees model the dynamics

of many biological processes. When the biological process originates from a common ancestor, the tree is *rooted*, where the root represents the common ancestor and is a unique node of degree 2. The evolution then progresses by series of bifurcations from the root (edges), ending in terminal nodes (leaves). Otherwise, the tree is unrooted.

Biologically, phylogenetic trees come from an input of molecular sequence data from a finite number of species. Given such sequence data, the task is then to reconstruct their evolutionary phylogeny and graphically represent it as a tree. Tree reconstruction is an extremely challenging problem that has been under active research for several decades. Techniques for tree reconstruction largely fall into two categories: statistical methods and distance-based methods.

Statistical methods are primarily based on the optimization of some specified optimality criteria, which are based on the idea that nucleotides in DNA evolution substitute one another according to a continuous-time Markov chain and generalized to an independent time-reversible model for finite sites (Tavaré, 1986). Classical statistical optimization methodology are then implemented, such as maximum parsimony or likelihood (Felsenstein, 1981; Fitch, 1971); Bayesian methods for tree reconstruction also exist to estimate the posterior distributions of trees (Edwards, 1970; Rannala and Yang, 1996). The underlying need for statistical methods is based on the fact that there is an extremely high number of possibilities for tree combinatorial types or *topologies* (i.e., the branching configuration together with a leaf labeling scheme): for rooted binary trees with  $N$  leaves, there are

$$(2N - 3)!! = (2N - 3) \times (2N - 5) \times \cdots \times 3$$

tree topologies (Schröder, 1870). The sample complexity for likelihood-based phylogenetic inference methods is known to match, up to constants, the information theoretic lower bound of classical models of evolution (Roch and Sly, 2017). For parsimony-based methods under the assumption of uniform distributivity, the optimization problem has been shown to be an NP-complete Steiner tree problem (Foulds and Graham, 1982). Restricted cases of the Steiner tree problem, such as the minimum spanning tree problem, as well as other variants are solvable in polynomial time and by other more efficient and scalable solutions (e.g., Juhl et al. (2018)). In biological applications when other distributional assumptions are reasonable, such as identifiability of mixture distributions, statistical methods are easier and more computationally efficient to implement (Allman and Rhodes, 2008; Long and Sullivant, 2015; Rhodes and Sullivant, 2012).

Distance-based methods deal with reconstructing trees from distance matrices (e.g., Fitch and Margoliash (1967); Saitou and Nei (1987); Sokal and Michener (1958)). These methods rely on the specification of genetic distances between all pairs of sequences, such as Hamming or Jukes–Cantor distances. Phylogenetic trees are then reconstructed from this matrix by positioning sequences that are closely related under the same node, with branch lengths faithfully corresponding to the observed distances between sequences. These pairwise distances between leaves in a tree can be stored in vectors, effectively representing trees as vectors. Such vectors computed from various trees can then be used for comparative statistical and computational studies on sets of trees. Other approaches that also represent trees as metrics have been studied where the tree itself is considered as a probability space arising from some stochastic process (on the sequence level), and Wasserstein distances as metrics on spaces of probability measures are then studied (Evans and Matsen, 2012; Sommerfeld and Munk, 2018).

We now provide the formal setting of phylogenetic trees in the context of distances; further details to supplement what follows may be found in Pachter and Sturmfels (2005).

**Notation** Throughout this paper,  $N \in \mathbb{N}$ , and we denote  $[N] := \{1, 2, \dots, N\}$  and  $n := \binom{N}{2}$ . We also write interchangeably  $w(i, j) = w_{ij} = w_{\{i, j\}}$ .

**Definition 3.** A *dissimilarity map*  $w$  is a function  $w : [N] \times [N] \rightarrow \mathbb{R}_{\geq 0}$  such that

$$w(i, i) = 0 \quad \text{and} \quad w(i, j) = w(j, i) \geq 0$$

for every  $i, j \in [N]$ . If a dissimilarity map  $w$  additionally satisfies the triangle inequality,  $w(i, j) \leq w(i, k) + w(k, j)$  for all  $i, j, k \in [N]$ , then  $w$  is called a *metric*.

The relationship between dissimilarity maps and metrics is intrinsically tropical.

**Lemma 4** (Butkovič (2010)). *Let  $w : [N] \times [N] \rightarrow \mathbb{R}_{\geq 0}$  be a dissimilarity map and let  $W$  be its corresponding matrix. Then  $w$  is a metric if and only if  $-W \odot -W = -W$ .*

### 2.2.1 Tree Metrics

For a tree with  $N$  leaves, the pairwise distances between leaves are sufficient to specify a phylogenetic tree.

**Definition 5.** Let  $T$  be a phylogenetic tree with  $N$  leaves, with labels  $[N]$ , and assign a branch length  $b_e \in \mathbb{R}_{\geq 0}$  to each edge  $e$  in  $T$ . Let

$$w : [N] \times [N] \rightarrow \mathbb{R}_{\geq 0}$$

$$w(i, j) \mapsto \bigoplus_{e \in P_{\{i, j\}}} b_e,$$

where  $P_{\{i, j\}}$  is the unique path from leaf  $i$  to leaf  $j$ . The map  $w$  is then called a *tree distance*. If  $w(i, j) \geq 0$  for all  $i, j \in [N]$ , then  $w$  is a *tree metric*.

Note that tree metrics may be represented as *cophenetic vectors* in the following manner (Cardona et al., 2013):

$$(w(1, 2), w(1, 3), \dots, w(N-1, N)) \in \mathbb{R}_{\geq 0}^n. \quad (1)$$

Cophenetic vectors are also called *tree metrics* (in vectorial representation) in the literature on mathematical phylogenetics. The following definition gives a technical condition for tree metrics.

**Definition 6.** The space  $\mathcal{T}_N$  of tree metrics for phylogenetic trees with  $N$  leaves consists of all  $n$ -tuples  $\{w(i, j)\}_{1 \leq i < j \leq N}$  where the maximum among the following tropically quadratic *Plücker relations*:

$$\begin{aligned} w(i, j) \odot w(k, l), \\ w(i, k) \odot w(j, l), \\ w(i, l) \odot w(j, k) \end{aligned} \quad (2)$$

is attained at least twice for  $1 \leq i < j < k < l \leq N$ . This condition for a tree metric is called the *four-point condition* (Buneman, 1974). This condition may equivalently be expressed as

$$w(i, j) \odot w(k, l) \leq w(i, k) \odot w(j, l) \boxplus w(i, l) \odot w(j, k) \quad (3)$$

for all distinct  $i, j, k, l \in [N]$ .

*Remark 7.* The space  $\mathcal{T}_N$  consists of all trees: by definition, in order to be a tree and an element of  $\mathcal{T}_N$ , it must satisfy the four-point condition. The four-point condition makes no distinction between rooted or unrooted trees; in the case of rooted trees, the root (i.e. leaf label 0) is simply ignored and the condition applies to the  $N$  leaves.

Notice that the conditions in Definition 6 are expressed in terms of maxima, which motivates our use of the max-plus convention in this work, as in Definition 1.

The four-point condition is a stronger constraint than the triangle inequality, and is the defining difference between a general metric and a tree metric. In other words, for a distance matrix to be a tree metric, it must satisfy not only the triangle inequality, but also the four-point condition. The implication is that general biological distance matrices do not necessarily give rise to phylogenetic trees: there may be biological processes with evolutionary behavior captured by distance matrices but that may not necessarily be realized as phylogenetic trees since not all distance matrices satisfy the four-point condition. We now give two examples to illustrate this distinction.

*Example 8.* Let  $N = 4$  and consider the matrix  $W$  with 0 on diagonal entries, and  $w(1, 2) = w(1, 3) = w(1, 4) = 1$ , and  $w(2, 3) = w(2, 4) = 1$ , but  $w(3, 4) = 2$ . Then

$$\begin{aligned} w(1, 2) \odot w(3, 4) &\not\leq w(1, 3) \odot w(2, 4) \boxplus w(1, 4) \odot w(2, 3) \\ w(1, 2) + w(3, 4) &\not\leq \max(w(1, 3) + w(2, 4), w(1, 4) + w(2, 3)) \\ 3 &\not\leq \max(2, 2) = 2. \end{aligned}$$

Thus, (3) is not satisfied, and it is therefore impossible to construct a phylogenetic tree with 4 leaves such that for  $1 \leq i < j \leq 4$ , the length of the unique path connecting leaves  $i$  and  $j$  is equal to  $w(i, j)$  as specified above.

*Example 9.* The tree metric  $w \in \mathbb{R}^6$  for the tree in Figure 1 expressed as a vector is  $(w_{PQ}, w_{PR}, w_{PS}, w_{QR}, w_{QS}, w_{RS})$ . As a matrix  $W$ , it is

$$\begin{pmatrix} 0 & w_{PQ} & w_{PR} & w_{PS} \\ & 0 & w_{QR} & w_{QS} \\ & & 0 & w_{RS} \\ & & & 0 \end{pmatrix} = \begin{pmatrix} 0 & a+b & a+c+d & a+c+e \\ & 0 & b+c+d & b+c+e \\ & & 0 & d+e \\ & & & 0 \end{pmatrix}.$$

The Plücker relations (2) associated with  $W$  are

$$\begin{aligned} A &:= w_{PQ} \odot w_{RS} = a + b + d + e, \\ B &:= w_{QR} \odot w_{PS} = a + b + 2c + d + e, \\ C &:= w_{PR} \odot w_{QS} = a + b + 2c + d + e. \end{aligned}$$

The maximum  $B = C$  is achieved exactly twice, and  $B - A = 2c > 0$ . Also, (3) holds:  $A \leq B \boxplus C = \max\{B, C\} = B$ .

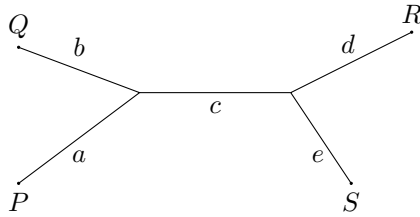


Figure 1: Example of an unrooted phylogenetic tree to illustrate the four-point condition.

### 2.2.2 Tree Ultrametrics

A strengthening of the triangle inequality for general metrics (see Definition 3) gives rise to an important class of tree metrics, which we will now discuss.

**Definition 10.** Let  $w : [N] \times [N] \rightarrow \mathbb{R}_{\geq 0}$  be a metric. If  $w(i, k) \leq w(i, j) \boxplus w(j, k)$  for each choice of distinct  $i, j, k \in [N]$ , then  $w$  is an *ultrametric*.

If  $w$  is a tree metric, and the maximum among

$$w(i, j), \quad w(i, k), \quad w(j, k),$$

is achieved at least twice for  $1 \leq i < j < k \leq N$ , then  $w$  satisfies the *three-point condition*, and hence is a *tree ultrametric* (Jardine et al., 1967). The space  $\mathcal{U}_N$  of tree ultrametrics for phylogenetic trees with  $N$  leaves consists of all  $n$ -tuples  $\{w(i, j)\}_{1 \leq i < j \leq N}$  satisfying the three-point condition for tree ultrametrics.

As in the case above for metrics to define tree metrics, the strengthening of the triangle inequality for a metric to an ultrametric applies to general metric functions, but analogously, in order for an ultrametric to be a tree ultrametric, it must satisfy the three-point condition. Trees satisfying the three-point condition imply also that the four-point condition is satisfied.

**Definition 11.** A rooted phylogenetic tree  $T$  with  $N$  leaves is called *equidistant* if the distance from every leaf to its root is a constant.

**Proposition 12.** A dissimilarity map computed from all pairwise distances between all pairs of leaves in a phylogenetic tree  $T$  is a tree ultrametric if and only if  $T$  is equidistant.

*Proof.* For any two points  $X, Y$  on a tree, we denote by  $w(X, Y)$  the length of the unique path connecting  $X$  and  $Y$ . Suppose a tree  $T$  is equidistant with root  $R$ . Then for any three leaves  $A, B, C$ , we have that  $w(R, A) = w(R, B) = w(R, C)$ . Since  $R, A, B, C$  satisfies the four-point condition, the maximum among (2):

$$w(R, A) + w(B, C), \quad w(R, B) + w(A, C), \quad w(R, C) + w(A, B),$$

is attained at least twice. Thus, the maximum among  $w(B, C), w(A, C), w(A, B)$  is also attained at least twice, satisfying the three-point condition, and  $T$  is therefore a tree ultrametric.

Conversely, suppose  $T$  is a tree ultrametric. Then there are finitely many leaves in  $T$ , so we can choose a pair of leaves  $A, B$  such that  $w(A, B)$  is maximal among all such pairs. Along the unique path from  $A$  to  $B$ , there is a unique point  $R$  such that  $w(R, A) = w(R, B)$ . For any other leaf  $C$ , consider the distance  $w(R, C)$ . Since the paths from  $R$  to  $A$  and  $B$  only intersect at  $R$ , the path from  $R$  to  $C$  intersects at least one of them only at  $R$ . Suppose without loss of generality that the path from  $R$  to  $A$  is such a path. Then  $w(A, C) = w(R, A) + w(R, C)$ . Since  $w(A, C) \leq w(A, B)$ , we have  $w(R, C) \leq w(R, B)$ . If  $w(R, C) < w(R, B)$ , then  $w(A, C) < w(R, A) + w(R, B) = 2w(R, B)$ , and  $w(B, C) \leq w(R, B) + w(R, C) < 2w(R, B)$ , so the maximum among  $w(A, B), w(A, C), w(B, C)$  is  $w(A, C) = 2w(R, B)$  and it is only attained once—a contradiction, since  $T$  was assumed a tree ultrametric. Hence,  $w(R, C) = w(R, B)$ , and  $R$  has equal distance to all leaves of  $T$ . Therefore  $T$  is equidistant with root  $R$ .  $\square$

### 2.2.3 The Tropical Projective Torus

Given that the three-point condition is stronger than the four-point condition, we have that the space of tree ultrametrics is contained in the space of tree metrics,  $\mathcal{U}_N \subset \mathcal{T}_N$ , which itself is a subset of the *tropical projective torus*. Denoted by  $\mathbb{R}^n/\mathbb{R}\mathbf{1}$ , it is the quotient space generated by the following equivalence relation  $\sim$  on  $\mathbb{R}^n$ :

$$x \sim y \Leftrightarrow x_1 - y_1 = x_2 - y_2 = \cdots = x_n - y_n.$$

In other words, for two points  $x, y \in \mathbb{R}^n$ ,  $x \sim y$  if and only if all coordinates of their difference  $x - y$  are equal. In the context of trees, the quotient normalizes evolutionary time between trees; tree distances differ from tree metrics by scalar multiples of  $\mathbf{1}$ , the vector of all ones.

The tropical projective torus  $\mathbb{R}^n/\mathbb{R}\mathbf{1}$  embeds into  $\mathbb{R}^{n-1}$  by considering representatives of the equivalence classes whose first coordinate is zero,  $(x_2 - x_1, x_3 - x_1, \dots, x_n - x_1) \in \mathbb{R}^{n-1}$ .

The tropical projective torus  $\mathbb{R}^n/\mathbb{R}\mathbf{1}$  may also be generated by a group action. Let  $G := \{(c, c, \dots, c) \in \mathbb{R}^n \mid c \in \mathbb{R}\}$  with coordinate-wise addition, then  $G$  is an additive group.  $G$  acts on  $\mathbb{R}^n$  as follows: for  $g \in G$  and  $x \in \mathbb{R}^n$ ,

$$g \circ x = (x_1 + g_1, x_2 + g_2, \dots, x_n + g_n).$$

Each point in  $\mathbb{R}^n/\mathbb{R}\mathbf{1}$  is then exactly one orbit under the group action of  $G$  on  $\mathbb{R}^n$ .

## 2.3 Some Common Tree Metrics

In this framework of tree metrics and ultrametrics, various metrics have been proposed to study distances between trees. The path difference, quartet distance, and Robinson–Foulds distance (or splits distance) are tree distances possessing the form of inner products of vectors, which makes them popular due to their integrability into a wide range of statistical approaches, such as functional and nonparametric modeling. However, they suffer from structural and interpretive problems: it turns out that many pairs of trees measure the same distance apart; also, large distances between trees do not signify large differences between shared ancestry of leaves (Steel and Penny, 1993). Other commonly-occurring distances include the nearest neighbor interchange metric (Waterman et al., 1976), subtree transfer distance (Allen and Steel, 2001), and variational distance (Steel and Székely, 2006). For a detailed survey and review of metrics between trees, see Weyenberg and Yoshida (2016); St. John (2016).

The cophenetic vectorization of tree metrics (1) represents trees as points in the Euclidean space  $\mathbb{R}^n$ , which may be compared using the cophenetic metric, which is simply the  $\ell^\infty$  distance (Cardona et al., 2013). In topological data analysis, the interleaving distance is constructed in the context of category theory and used to compare persistence modules. Recent work by Munch and Stefanou (2019) shows that the  $\ell^\infty$ -cophenetic metric is in fact an interleaving distance, connecting the fields of mathematical phylogenetics and topological data analysis.

### 2.3.1 The BHV Geodesic Metric

A pioneering contribution to the study of sets of phylogenetic trees is due to Billera, Holmes, and Vogtmann, who introduced a moduli space that considers equidistant rooted phylogenetic trees on a fixed set of leaves as points with geometry characterized by geodesics (Billera et al., 2001). Due to its intuitive and elegant construction, which then results in desirable properties of the geodesic, BHV space has been suggested and proposed as the decisive setting for statistics on phylogenetic tree space (Benner et al., 2014; Gavryushkin and Drummond, 2016). This metric and the space in which it lives are particularly relevant to our work; we describe them in greater detail, since much of the contributions presented in this paper are comparative to the BHV setting.

In BHV space, trees are expressed only by the lengths of their internal edges. External edges are not considered, since taking them into account does not affect the geometry of the space: including external edges simply amounts to taking the product of tree space with an  $N$ -dimensional Euclidean space. Any two points (i.e., two rooted trees with a fixed set of leaves) are connected by a geodesic, with the distance between the points being defined by the length of the distance connecting them. In this paper, we denote the BHV space of trees with  $N$  leaves by  $\mathcal{T}_N^{\text{BHV}}$ , and the case where rooted phylogenetic trees with  $N$  leaves with zero-length external edges and finite branch lengths from the root to the leaves are normalized to length 1 by  $\mathcal{U}_N^{\text{BHV}} \subset \mathcal{T}_N^{\text{BHV}}$ . The latter case of  $\mathcal{U}_N^{\text{BHV}}$  is also widely studied (e.g., Gavryushkin and Drummond (2016), Section 5 of Holmes (2003), and Lin et al. (2017)), including in Section 4.4 of the original paper by Billera et al. (2001). The  $\mathcal{U}_N^{\text{BHV}}$  standardization to unit edge lengths presents only a mild simplification of the geometry of  $\mathcal{T}_N^{\text{BHV}}$  (Holmes, 2003).

The construction of BHV space proceeds as follows: Consider a rooted tree with  $N$  leaves. Such a tree has at most  $2N - 2$  edges:  $N$  terminal edges, which are connected to leaves, and at most  $N - 2$  internal edges. When a rooted tree is *binary* (that is, it is a bifurcating tree that has exactly two descendants stemming from each interior node), then the number of edges is exactly  $N - 2$ ; the number of edges is lower than  $N - 2$  if it is not binary. To each distinct tree combinatorial type or topology, a Euclidean orthant of dimension  $N - 2$  (i.e., the number of internal edges) is associated. An orthant may be regarded as the polyhedral cone of  $\mathbb{R}^{N-2}$  where all coordinates are nonnegative. Thus, for each tree topology, the orthant coordinates correspond to the internal edge lengths in the tree. The orthant *boundaries* (where at least one coordinate is zero) represent trees with collapsed internal edges. These points can be thought of as trees with slightly different, though closely related, tree topologies. The BHV space is constructed by noting that the boundary trees from two different orthants may describe the same polytomic topology (i.e., a *split*) and thus grafting orthant boundaries together when the trees they represent coincide. The grafting of orthants always occurs at right-angles. Note that an equivalent construction may also be outlined for  $N - 3$  internal edges for the case of unrooted trees.

Geodesics are unique in BHV space: the right-angle grafting of cones characterizes the curvature of the space so that it satisfies the CAT(0) property of flag complexes, and the uniqueness of geodesics immediately follows. To compute a geodesic in  $\mathcal{T}_N^{\text{BHV}}$ , first, the geodesic distance between two trees on the BHV tree space is computed, and then the terminal branch lengths are considered to compute the overall geodesic distance between two trees, by taking the differences between terminal branch lengths. Since each orthant is locally viewed as a Euclidean space, the shortest path between two points within a single orthant is a straight Euclidean line. The difficulty appears in establishing which sequence of orthants joining the two topologies contains the geodesic. In the case of four leaves, this can be readily determined using a systematic grid search, but such a search is intractable with larger trees. Owen and Provan (2011) present a quartic-time algorithm (in the number of leaves  $N$ ) for finding the geodesic path between any two points in BHV space, which is the currently the fastest available method with a time complexity of  $O(N^4)$ .

## 2.4 Relating Tropical Geometry to Phylogenetic Tree Space

The connection of tropical geometry to phylogenetic tree space arises in two occurrences. Classically, as discussed in Maclagan and Sturmfels (2015), the space of phylogenetic trees with  $N$  leaves is the moduli space of tropical curves of genus 0 and  $N$  marked points. A more recent result upon which our work is based identifies a homeomorphism between the space of phylogenetic trees with  $N$  leaves and a tropical construction of the Grassmannian of 2-planes in  $N$  dimensions (Speyer and Sturmfels, 2004). The Grassmannian is the space of all  $k$ -dimensional subspaces of an  $n$ -dimensional vector space, with  $k < n$ , which can be mapped to a

*projective variety*—a particular zero set of polynomials—via a construction known as the *Plücker embedding*. Tropicalizing the Plücker embedding for the Grassmannian of 2-planes in  $N$  dimensions recovers the four-point condition (see Definition 6) explicitly describing phylogenetic trees with  $N$  leaves as tree metrics. Essentially, this result endows the space of phylogenetic trees with a tropical structure: the homeomorphism provides a purely tropical parameterization of the space of phylogenetic trees via the Plücker relations given in Definition 6. In this work, we study characteristics of this tropical structure for computational and especially data analytic applications involving sets of phylogenetic trees.

### Other Applications of Tropical Geometry

Tropical geometry also arises in other applied settings, specifically in computer science, statistics, and economics: Maclagan and Sturmfels (2015) and Pachter and Sturmfels (2005) discuss the use of tropical mathematics to reinterpret the dynamic programming approach to the problem of sequence alignment for molecular data in computational biology. In the context of statistics, tropical geometry arises in the reinterpretation of various stochastic models. As a field of research, one of the core principles of algebraic statistics is the fact that algebraic varieties and semi-algebraic sets are statistical models (Améndola et al., 2018; Sullivant, 2018). For statistical models, such as graphical models, tropicalized statistical models (i.e., tropicalized algebraic varieties) are fundamental in parametric inference, which was specifically demonstrated on hidden Markov models and general Markov models on binary trees (Pachter and Sturmfels, 2004). In computational biology, this algebraic statistical approach was adapted to study invariants of joint probability distributions on leaf labels of phylogenetic trees (Sturmfels and Sullivant, 2005). In economics and finance, tropical geometry arises in game theoretic settings and max-linear models for financial data (Einmahl et al., 2018; Lin and Tran, 2019).

## 3 Palm Tree Space

Our main contribution in this section is a metric measure space construction for the set of all phylogenetic trees. Here, we prove geometric, topological, and analytic properties of the space that are not only desirable for computation, but also turn out to result in probabilistic and statistical advantages. We also give a comparison of these properties relative to BHV space. We begin by motivating our study.

### 3.1 Motivation: Statistics in BHV Space

While results enabling statistical analysis on BHV space exist (e.g., Benner et al. (2014); Holmes (2005)), they are not always straightforward to implement nor interpret. There are two important reasons underlying these difficulties. First, polytopes in BHV space with edges defined by geodesics—where the geodesics are calculated by currently the fastest available and most widely used algorithm (Owen and Provan, 2011)—are unbounded in dimension (Lin et al., 2017). In the most general case, these can be polytopes whose edges are all cone paths, which have maximal *depth*: The depth of a point  $x$  in the relative interior of some  $k$ -dimensional polyhedron is the codimension of the polyhedron,  $N - 2 - k$ ; the depth of a geodesic is the largest depth among all points on the geodesic, or, in other words, the largest codimension among all cones traversed.

**Corollary 13** (Lin et al. (2017)). *There exist three ultrametric trees with  $2d + 2$  leaves whose geodesic triangle in ultrametric BHV space  $\mathcal{U}_{2d+2}^{\text{BHV}}$  has dimension at least  $d$ ,  $d \geq 1$ .*

The statistical implication of this result is that there exist no useful, lower-dimensional representations (projections) of data on BHV planes. This is restrictive for classical dimensionality reduction and data visualization methods, such as principal component analysis (PCA). Sophisticated methods have since been developed to bypass these limitations (Feragen et al., 2013; Nye, 2011; Nye et al., 2017).

Large depths of geodesics also give rise to the phenomenon of *stickiness* (Miller et al., 2015), where the Fréchet mean lies stably at a singularity on a lower-dimensional orthant, and perturbing any of the data points results in no change in the mean; see Example 15. The statistical implication here is that there exists no exact asymptotic distribution for the mean.

**Definition 14** (Stephan Huckemann, personal communication). Let  $\mathcal{M}$  be a space of probability measures on a topological space  $Q$ , and suppose that  $\mathcal{M}$  is endowed with a topology. Further, consider a map  $E : \mathcal{M} \rightarrow \mathbf{Q}$  to closed subsets of  $Q$ . Then a measure  $\mu \in \mathcal{M}$  is said to *stick* to a set  $M \subseteq Q$  if  $E(\mu) = M$ , and for every neighborhood  $U'$  of  $\mu$  in  $\mathcal{M}$ , there is an open subset  $U \subset U'$  such that  $E(\nu) \subseteq M$  for all  $\nu \in U$ .

*Example 15.* In Figure 2, we position three unit masses on the 3-spider, which is the stratified space of three  $\mathbb{R}_{\geq 0}$  rays joined at the origin. This is precisely the BHV space of phylogenetic trees with three leaves and fixed pendant edge lengths, since, as mentioned previously, coordinates in BHV space are given only by internal edge lengths. The position  $x$  of the barycenter (Fréchet mean) is calculated by minimizing  $2(1+x)^2 + (a-x)^2$ . The solution is  $x = 0$  for  $a < 2$ , and  $x = (a-2)/3$  for  $a \geq 2$ . The Fréchet mean tends to stick to lower-dimensional strata.

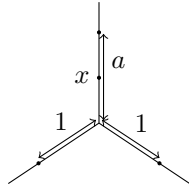


Figure 2: 3-spider to illustrate stickiness.

This phenomenon has been well studied in various settings, including BHV space in particular (Barden and Le, 2018; Hotz et al., 2013), but also in more general settings of hyperbolic planar singularities (Huckemann et al., 2015). The strategy used to bypass this difficulty is to obtain approximations using the delta method to derive asymptotic behavior and yield a central limit theorem (Barden et al., 2013). Approximate and nonparametric approaches for inference have then been proposed based on this strategy; e.g., Willis (2019); Willis and Bell (2018).

These limitations given by the maximal depth property of BHV space have been the motivation for the recent work adopting the tropical interpretation of tree space (Lin et al., 2017; Yoshida et al., 2019). Our contribution in the present paper is a formal study of mathematical properties of the metric geometry of this interpretation, and specifically, those that give rise to desirable settings for studies in probability and statistics.

### 3.2 The Tropical Metric

Endowing the tropical projective torus  $\mathbb{R}^n/\mathbb{R}\mathbf{1}$  with a generalized Hilbert projective metric function (Akian et al., 2011; Cohen et al., 2004) results in a metric space, which we now define and study. This metric is tropical and combinatoric in nature, and has been used in recent literature on tropical geometric tree spaces (Lin et al., 2017; Yoshida et al., 2019).

**Definition 16.** For any point  $x \in \mathbb{R}^n$ , denote its coordinates  $x_1, x_2, \dots, x_n$  and its representation in  $\mathbb{R}^n/\mathbb{R}\mathbf{1}$  by  $\bar{x}$ . For  $\bar{x}, \bar{y} \in \mathbb{R}^n/\mathbb{R}\mathbf{1}$ , set the distance between  $\bar{x}$  and  $\bar{y}$  to be

$$\begin{aligned} d_{\text{tr}}(\bar{x}, \bar{y}) &:= \max_{1 \leq i < j \leq n} |(x_i - y_i) - (x_j - y_j)| \\ &= \max_{1 \leq i \leq n} (x_i - y_i) - \min_{1 \leq i \leq n} (x_i - y_i). \end{aligned}$$

We refer to the function  $d_{\text{tr}}$  as the *tropical metric*.

**Proposition 17.** *The function  $d_{\text{tr}}$  is a well-defined metric function on  $\mathbb{R}^n/\mathbb{R}\mathbf{1}$ .*

*Proof.* We verify that the defining properties of metrics are satisfied. By definition, for  $u, v \in \mathbb{R}^n$ ,  $d_{\text{tr}}(\bar{u}, \bar{v}) = d_{\text{tr}}(\bar{v}, \bar{u})$ , satisfying symmetry. The tropical metric is nonnegative, since  $|(u_i - v_i) - (u_j - v_j)| \geq 0$ , so is  $d_{\text{tr}}(\bar{u}, \bar{v}) \geq 0$ . If  $d_{\text{tr}}(\bar{u}, \bar{v}) = 0$ , then  $u_i - v_i$  are equal for all  $1 \leq i \leq n$ , thus  $\bar{u} = \bar{v}$ , so indiscernibles are identifiable.

For  $u, v, w \in \mathbb{R}^n$ , we now show that triangle inequality is satisfied:  $d_{\text{tr}}(\bar{u}, \bar{w}) \leq d_{\text{tr}}(\bar{u}, \bar{v}) + d_{\text{tr}}(\bar{v}, \bar{w})$ . Suppose  $1 \leq i' < j' \leq n$  such that

$$|(u_{i'} - w_{i'}) - (u_{j'} - w_{j'})| = \max_{1 \leq i < j \leq n} |u_i - w_i - u_j + w_j|,$$

then  $d_{\text{tr}}(\bar{u}, \bar{w}) = |u_{i'} - w_{i'} - u_{j'} + w_{j'}|$ . Note that

$$u_{i'} - w_{i'} - u_{j'} + w_{j'} = (u_{i'} - v_{i'} - u_{j'} + v_{j'}) + (v_{i'} - w_{i'} - v_{j'} + w_{j'}).$$

Hence

$$\begin{aligned} d_{\text{tr}}(\bar{u}, \bar{w}) &= |u_{i'} - w_{i'} - u_{j'} + w_{j'}| \leq |u_{i'} - v_{i'} - u_{j'} + v_{j'}| + |v_{i'} - w_{i'} - v_{j'} + w_{j'}| \\ &\leq d_{\text{tr}}(\bar{u}, \bar{v}) + d_{\text{tr}}(\bar{v}, \bar{w}). \end{aligned}$$

Thus,  $d_{\text{tr}}$  is a metric function on  $\mathbb{R}^n/\mathbb{R}\mathbf{1}$ . □

With this metric, we formally define palm tree space as follows.

**Definition 18.** For a positive integer  $N$ , let  $\mathcal{T}_N$  be the space of phylogenetic trees as in Definition 6. The metric space  $\mathcal{P}_N := (\mathcal{T}_N, d_{\text{tr}})$  is called the *palm tree space*.

*Remark 19.* Palm tree space is defined in the general setting of non-equidistant trees (see Definition 11), where the rootedness of the trees is not a significant matter. When there is no condition of equidistance, there is no constraint on pairwise distances between leaves in the tree and thus any point in the tree may be treated as a root. In other words, palm tree space may be defined generally, in terms of either rooted or unrooted non-equidistant trees.

The spaces  $\mathcal{T}_N^{\text{BHV}}$  and  $\mathcal{P}_N$  are not isometric, meaning that absolute lengths measured by each metric are not consistent. To understand the variation in length discrepancy, we study the stability of the tropical metric  $d_{\text{tr}}$  and find that perturbations of points in BHV space, measured by the BHV metric  $d_{\text{BHV}}$ , correspond to bounded perturbations of their images in palm tree space, measured by the tropical metric. This stability property is desirable, since it allows for interpretable comparisons between the two spaces, and allows for “translations” in the widely-used BHV framework over to palm tree space.

The following lemma ensures coordinate-wise stability of the tropical metric in  $\mathcal{P}_N$ .

**Lemma 20.** *Let  $u \in \mathbb{R}^n$ . For  $1 \leq i \leq n$ , if we perturb the  $i$ th coordinate of  $u$  by  $\varepsilon$  to obtain another point  $u' \in \mathbb{R}^n$ , then in  $\mathbb{R}^n/\mathbb{R}\mathbf{1}$  we have*

$$d_{\text{tr}}(\bar{u}, \bar{u}') = |\varepsilon|.$$

*Proof.* For  $1 \leq j \leq n$ , the difference  $u'_j - u_j = 0$  if  $j \neq i$ , and  $u'_i - u_i = \pm\varepsilon$ . The set of these differences is then either  $\{0, \varepsilon\}$  or  $\{0, -\varepsilon\}$ . By Definition 16,  $d_{\text{tr}}(\bar{u}, \bar{u}') = |0 - \pm\varepsilon| = |\varepsilon|$ . □

**Theorem 21 (Stability).** *Let  $N$  be the number of leaves in palm tree space and BHV space. Let  $u$  and  $u'$  be two unrooted phylogenetic trees with  $N$  leaves. Then the following inequality holds:*

$$d_{\text{tr}}(u, u') \leq \sqrt{N+1} \cdot d_{\text{BHV}}(u, u').$$

*Moreover, the smallest possible constant is  $\sqrt{N+1}$ .*

*Proof.* We first prove that for any two unrooted trees  $u, u'$  with  $N$  leaves,  $d_{\text{tr}}(u, u') \leq \sqrt{N+1} \cdot d_{\text{BHV}}(u, u')$ . First, assume that  $u, u'$  belong to the same orthant in BHV space. Then no matter what the tree topology is, if we denote the differences of the lengths of the  $N-3$  internal edges in  $u$  and  $u'$  by  $d_1, d_2, \dots, d_{N-3}$ , and the differences of the length of the  $N$  external edges by  $p_1, p_2, \dots, p_N$ , we always have

$$d_{\text{BHV}}(u, u') = \sqrt{\sum_{i=1}^{N-3} d_i^2 + \sum_{i=1}^N p_i^2}$$

(e.g., Lin et al. (2017); Owen and Provan (2011)).

For every pair of leaves  $i, j$  in both trees, the distance between them is a sum of the length of some internal edges and two external edges. In other words, all differences  $w_{\{i,j\}}^u - w_{\{i,j\}}^{u'}$  are of the form of the sum between some  $d_k$ , and  $p_i + p_j$ . Thus, the maximum of these differences is at most the sum of all positive  $d_i$  values, plus the two greatest  $p_i$  values (take these to be  $p_{i_1}$  and  $p_{i_2}$ ), while the minimum of these differences is at least the sum of all negative  $d_i$  values, plus two smallest  $p_i$  values (take these to be  $p_{i_3}$  and  $p_{i_4}$ ). By definition,  $d_{\text{tr}}(u, u')$  is the maximum minus the minimum of these differences, so we have

$$d_{\text{tr}}(u, u') \leq \sum_{i=1}^{N-3} |d_i| + |p_{i_1}| + |p_{i_2}| + |p_{i_3}| + |p_{i_4}|.$$

By the Cauchy–Schwarz inequality (Cauchy, 1821; Schwarz, 1890),

$$(N+1) \cdot \left( \sum_{i=1}^{N-3} |d_i|^2 + |p_{i_1}|^2 + |p_{i_2}|^2 + |p_{i_3}|^2 + |p_{i_4}|^2 \right) \geq \left( \sum_{i=1}^{N-3} |d_i| + \sum_{i=1}^N |p_i| \right)^2.$$

Hence

$$\begin{aligned} d_{\text{tr}}(u, u') &\leq \sum_{i=1}^{N-3} |d_i| + |p_{i_1}| + |p_{i_2}| + |p_{i_3}| + |p_{i_4}| \\ &\leq \sqrt{N+1} \cdot \sqrt{\sum_{i=1}^{N-3} |d_i|^2 + |p_{i_1}|^2 + |p_{i_2}|^2 + |p_{i_3}|^2 + |p_{i_4}|^2} \\ &\leq \sqrt{N+1} \cdot \left( \sum_{i=1}^{N-3} |d_i|^2 + \sum_{i=1}^N p_i^2 \right) \\ &= \sqrt{N+1} \cdot d_{\text{BHV}}(u, u'). \end{aligned}$$

Now, for  $u, u'$  with distinct tree topologies, we consider the unique geodesic connecting them: there exist finitely many points  $u^1, \dots, u^{k-1}$  in BHV space such that  $u^i$  and  $u^{i+1}$  belong to the same polyhedron corresponding to a tree topology for  $0 \leq i \leq k-1$ , where  $u^0 = u$  and  $u^k = u'$ , and  $d_{\text{BHV}}(u, u') = \sum_{i=0}^{k-1} d_{\text{BHV}}(u^i, u^{i+1})$ . For  $1 \leq i \leq k-1$ , by the proof above, we have that

$$d_{\text{tr}}(u^i, u^{i+1}) \leq \sqrt{N+1} \cdot d_{\text{BHV}}(u^i, u^{i+1}) \quad \forall \quad 1 \leq i \leq k-1.$$

Thus,

$$d_{\text{tr}}(u, u') \leq \sum_{i=0}^{k-1} d_{\text{tr}}(u^i, u^{i+1}) \leq \sum_{i=0}^{k-1} \sqrt{N+1} \cdot d_{\text{BHV}}(u^i, u^{i+1}) = \sqrt{N+1} \cdot d_{\text{BHV}}(u, u').$$

Next, we consider the case where the equality holds: consider two trees  $T_1$  and  $T_2$  with  $N$  leaves and the same tree topology, given by the following nested sets

$$\{\{1, 2\}, \{1, 2, 3\}, \dots, \{1, 2, \dots, N-2\}\}.$$

Suppose in  $T_1$ , the internal edges have lengths

$$b^1(e_i) = \begin{cases} 2, & \text{if } 1 \leq i \leq N-4; \\ 1, & \text{if } i = N-3. \end{cases}$$

Similarly, in  $T_2$ , the internal edges have lengths

$$b^2(e_i) = \begin{cases} 1, & \text{if } 1 \leq i \leq N-4; \\ 2, & \text{if } i = N-3. \end{cases}$$

The external edge lengths of  $T_1$  and  $T_2$  are

$$p_j^i = \begin{cases} 1, & \text{if } (i, j) = (1, 2), (1, N-2), (2, N-1), (2, N); \\ 0, & \text{otherwise.} \end{cases}$$

Then

$$d_{\text{BHV}}(T_1, T_2) = \sqrt{(N-4) \cdot (2-1)^2 + (1-2)^2 + 2 \cdot (1-0)^2 + 2 \cdot (0-1)^2} = \sqrt{N+1}.$$

For  $1 \leq i < j \leq N$ , in either tree the distance  $w_{\{i,j\}}$  is the sum of the edge lengths of

$$p_i, e_{\max(i-1,1)}, e_{\max(i-1,1)+1}, \dots, e_{\max(j-2, N-3)}, p_j.$$

Since  $b^1(e_i) > b^2(e_i)$  for  $i < N-3$  and  $b^1(e_i) < b^2(e_i)$  for  $i = N-3$ , the maximum of all differences  $w_{\{i,j\}}^1 - w_{\{i,j\}}^2$  is

$$w_{\{2, N-2\}}^1 - w_{\{2, N-2\}}^2 = ((N-4) \cdot 2 + 2 \cdot 1) - (N-4) \cdot 1 = N-2;$$

and the minimum of all differences  $w_{\{i,j\}}^1 - w_{\{i,j\}}^2$  is

$$w_{\{N-2, N-1\}}^1 - w_{\{N-2, N-1\}}^2 = 1 - (2 + 1 + 1) = -3.$$

By definition,  $d_{\text{tr}}(T_1, T_2) = (N-2) - (-3) = N+1 = \sqrt{N+1} \cdot d_{\text{BHV}}(T_1, T_2)$  in this case. Thus,  $\sqrt{N+1}$  is the smallest possible stability constant.  $\square$

In general, and especially data applications, the number of leaves is fixed prior to the study so the stability constant  $\sqrt{N+1}$  is indeed a constant.

*Remark 22.* It is important to note here that explicit calculations involving geodesics between trees in the original paper by Billera et al. (2001) do not include external edges, since these do not modify the geometry of the space. Indeed, their inclusion only amounts to an additional Euclidean factor, since the tree space then becomes the cross product of BHV space of trees with internal edges only, and  $\mathbb{R}_{\geq 0}^N$ . Geodesic distances, which depend directly on geodesic paths (the former is the length of the latter), considered in Billera et al. (2001) also do not include pendant edges.

The statement of Theorem 21 treats the most general case of unrooted trees with pendant edges included in both tree spaces. Our reasoning for considering this case, which differs from what appears in Billera et al. (2001) as described above, is twofold. First, the procedure for calculating geodesic distances between trees in BHV space follows Owen and Provan (2011), who explicitly consider pendant edges in computing geodesics, and whose algorithm is considered to be the current standard. Since the tropical metric includes pendant edges in its calculation, a study relative to the Owen–Provan algorithm Owen and Provan (2011), rather than the procedure given in Billera et al. (2001) where pendant edges are excluded, provides a more valid comparison. Second, our work builds upon previous studies on the tropical metric in Lin et al. (2017) that also deals with comparative studies relative to the Owen–Provan algorithm. We follow in this same vein for consistency.

In terms of interpretation, Theorem 21 provides an important comparative measure and guarantees that quantitative results from BHV space are bounded in palm tree space. For example, in single-linkage clustering, where clusters are fully determined by distance thresholds, the stability result means that a given clustering pattern in BHV space will be preserved in palm tree space, thus maintaining interpretability of clustering behavior.

### 3.3 Geometry of Palm Tree Space

The uniqueness property of geodesics in BHV space, used in the proof of Theorem 21, leads naturally to the study of similar geometric properties that characterize palm tree space as well as important differences between the two spaces. These characteristics will now be developed in this section.

### 3.3.1 Geodesics in Palm Tree Space

**Definition 23.** A *geodesic* between any two points  $x$  and  $y$  in a metric space is a path between  $x$  and  $y$  with the shortest length (measured by the metric) that is fully contained within the metric space.

In palm tree space, geodesics are in general not unique, which is a common occurrence in various metric spaces. There exists, however, a unique path joining two points in palm tree space, which is also a geodesic—the tropical line segment.

**Definition 24.** Given  $x, y \in \mathbb{R}^n / \mathbb{R}\mathbf{1}$ , the *tropical line segment* with endpoints  $x$  and  $y$  is the set

$$\{a \odot x \boxplus b \odot y \in \mathbb{R}^n / \mathbb{R}\mathbf{1} \mid a, b \in \mathbb{R}\}.$$

Here, max-plus addition  $\boxplus$  for two vectors is performed coordinate-wise.

**Proposition 25.** For points  $x, y \in \mathcal{P}_N$ , the tropical line segment connecting  $x$  and  $y$  is a geodesic.

*Proof.* It suffices to show that for any  $a, b \in \mathbb{R}$ , we have that

$$d_{\text{tr}}(z, x) + d_{\text{tr}}(z, y) = d_{\text{tr}}(x, y),$$

where  $z = a \odot x \boxplus b \odot y$  is the tropical line segment. We may assume that  $x_i - y_i \leq x_{i+1} - y_{i+1}$  for  $1 \leq i \leq n-1$ . Under this assumption,  $d_{\text{tr}}(x, y) = (x_n - y_n) - (x_1 - y_1)$ . Now if  $0 \leq j \leq n$  is the largest index such that  $x_j - y_j \leq b - a$ , then for some  $i \geq j+1$ ,  $z_i = b + y_i$  and, analogously,  $z_i = a + x_i$ . If  $j = 0$  or  $j = n$ , then  $z$  is equal to either  $x$  or  $y$  and the claim is apparent. We may thus assume  $1 \leq j \leq n-1$ .

The set of all differences  $x_i - z_i$  contains  $-a$  and the greater values  $x_i - y_i - b > -a$  for  $i \geq j+1$ . So,

$$d_{\text{tr}}(z, x) = (x_n - y_n - b) - (-a) = (x_n - y_n) + (a - b).$$

Similarly, the set of all differences  $z_i - y_i$  contains  $b$  and the smaller values  $(x_i - y_i) + a < b$  for  $i \leq j$ . So,

$$d_{\text{tr}}(z, y) = b - (x_1 - y_1 + a) = (b - a) - (x_1 - y_1).$$

Therefore,  $d_{\text{tr}}(z, x) + d_{\text{tr}}(z, y) = d_{\text{tr}}(x, y)$ , and the tropical line segment connecting  $x$  and  $y$  is a geodesic.  $\square$

In addition, it turns out that tropical line segments are easy and fast to compute. In particular, the time complexity to compute them is lower than that of the Owen–Provan algorithm, which is currently the fastest available algorithm to compute the unique geodesics in BHV space with a time complexity of  $O(N^4)$ .

**Proposition 26.** (Maclagan and Sturmfels, 2015, Proposition 5.2.5) The time complexity to compute the tropical line segment connecting two points in  $\mathbb{R}^n / \mathbb{R}\mathbf{1}$  is  $O(n \log n) = O(N^2 \log N)$ .

### 3.3.2 Structure of Palm Tree Space

In the same way that  $\mathcal{T}_N^{\text{BHV}}$  is constructed as the union of polyhedra, the geometry of  $\mathcal{P}_N$  is also given by such a union.

**Proposition 27.** (Maclagan and Sturmfels, 2015, Proposition 4.3.10) The space  $\mathcal{T}_N$  is the union of  $(2N-5)!!$  polyhedra in  $\mathbb{R}^n / \mathbb{R}\mathbf{1}$  with dimension  $N-3$ .

Here, the cone in consideration is the usual convex cone as a subset of a vector space on an ordered field, closed under linear combinations with positive coefficients.

## 3.4 Topology of Palm Tree Space

The measure of a space is relevant in probabilistic studies; the measure of a topological space, in particular, results in a desirable compatibility where the topology of a space may be interpreted in terms of measures. For example, Radon measures may also be interpreted as linear functionals on the space of continuous functions with compact support, which is locally convex, by e.g., Bourbaki (2004), Chapter 3. This motivates our study of the topology of palm tree space.

The following two lemmas allow us to characterize the topology of palm tree space. Recall that for  $x \in \mathbb{R}^n$ , the set  $B(x, r) = \{y \in \mathbb{R}^n \mid |y - x| < r\}$  is the open ball centered at  $x$  with radius  $r$ . By identifying  $\mathbb{R}^n/\mathbb{R}\mathbf{1}$  with  $\mathbb{R}^{n-1}$  as discussed in Section 2.2.3, an equivalent set may be correspondingly defined in palm tree space as follows.

**Definition 28.** Under the tropical metric  $d_{\text{tr}}$ , we define  $B_{\text{tr}}(x, r) = \{y \in \mathbb{R}^n \mid d_{\text{tr}}((0, \bar{y}), (0, \bar{x})) < r\}$  to be the open *tropical ball* centered at  $x$  with radius  $r$ .

**Lemma 29.** For  $x \in \mathbb{R}^{n-1}$  and  $r > 0$ , the open tropical ball  $B_{\text{tr}}(x, r)$  is the open convex polytope defined by the following strict inequalities for  $1 \leq i < j \leq n - 1$ :

$$\begin{aligned} y_i &> x_i - r, \\ y_i &< x_i + r, \\ y_i - y_j &> x_i - x_j - r, \\ y_i - y_j &< x_i - x_j + r. \end{aligned} \tag{4}$$

*Proof.* For  $y \in \mathbb{R}^{n-1}$ ,  $y \in B_{\text{tr}}(x, r)$  if and only if  $d_{\text{tr}}((0, \bar{x}), (0, \bar{y})) < r$ . Definition 16 admits the strict inequalities in (4).  $\square$

**Lemma 30.** For  $r > 0$  and  $x \in \mathbb{R}^{n-1}$ ,  $B(x, r) \subseteq B_{\text{tr}}(x, 2r)$  and  $B_{\text{tr}}(x, r) \subseteq B(x, \sqrt{n-1}r)$ .

*Proof.* By Lemma 29, if a point  $y$  lies in  $B_{\text{tr}}(x, r)$ , then for  $1 \leq i \leq n-1$ ,  $|y_i - x_i| < r$ , thus  $y \in B(x, \sqrt{n-1}r)$ . Conversely, if a point  $y$  lies in  $B(x, r)$ , then for  $1 \leq i \leq n-1$ , we have that  $|y_i - x_i| < r$ . Therefore,

$$|(y_i - y_j) - (x_i - x_j)| = |(y_i - x_i) - (y_j - x_j)| < 2r.$$

Hence  $y \in B_{\text{tr}}(x, 2r)$ .  $\square$

**Theorem 31.** On  $\mathbb{R}^{n-1}$ , the family of open balls  $B(x, r)$  and the family of open tropical balls  $B_{\text{tr}}(x, r)$  define the same topology.

*Proof.* Suppose for all  $r > 0$  and  $x \in \mathbb{R}^{n-1}$  that the open balls  $B(x, r)$  form a topological basis. For any  $y \in \mathbb{R}^{n-1}$  and  $s > 0$ , we consider the ball  $B_{\text{tr}}(y, s)$ : For any point  $z \in B_{\text{tr}}(y, s)$ , we have that  $d_{\text{tr}}(z, y) < s$ . Let  $\varepsilon = \frac{s - d_{\text{tr}}(z, y)}{2} > 0$ . Then  $B_{\text{tr}}(z, 2\varepsilon) \subseteq B_{\text{tr}}(y, s)$ . By Lemma 30, we have  $B(z, \varepsilon) \subseteq B_{\text{tr}}(z, 2\varepsilon) \subseteq B_{\text{tr}}(y, s)$ . Therefore,  $B_{\text{tr}}(y, s)$  is also an open set. The other direction is proved in the same manner.  $\square$

*Example 32.* Figure 3 illustrates the unit balls in Euclidean, BHV, and palm tree space. Here, the number of leaves is fixed to be 3. There are three 1-dimensional cones in BHV space, and they share the origin. The palm tree space  $\mathcal{P}_3 = \{w = (w_{\{1,2\}}, w_{\{1,3\}}, w_{\{2,3\}}) \in \mathbb{R}^3/\mathbb{R}\mathbf{1} \mid \max(w) \text{ is attained at least twice}\}$  may be embedded in  $\mathbb{R}^2$ .

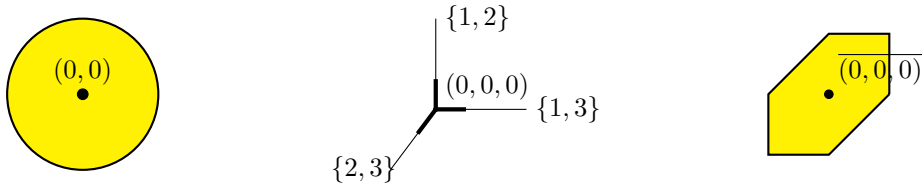


Figure 3: Comparison of unit balls in Euclidean, BHV, and palm tree space for  $N = 3$  leaves. The leftmost figure is the Unit ball  $B((0,0), 1)$  in  $\mathbb{R}^2$ ; the center figure is the unit ball centered at the origin with radius 1 in a BHV space with 3 leaves; the rightmost figure is the unit ball  $B_{\text{tr}}((0,0,0), 1)$  in  $\mathcal{P}_3$ .

### 3.5 Palm Tree Space is a Polish Space

We have thus far established palm tree space as a metric space when equipped with the tropical metric, and moreover, established its topology. We now prove additional analytic properties of palm tree space that are desirable for probabilistic and statistical analysis. Specifically, we prove that palm tree space is a separable, completely metrizable topological space, and thus a Polish space, by definition.

Polish spaces are important settings for studies in probability due to the fact that classical results maybe formulated and generalized in a well-behaved manner; some examples are the construction of conditional expectations, Kolmogorov's extension theorem (which guarantees the definition of a stochastic process from a series of finite-dimensional distributions), and Prokhorov's theorem (which guarantees weak convergence by relating tightness of measures to compactness in a probability space) (Parthasarathy, 1967).

**Proposition 33.**  $\mathcal{P}_N$  is complete.

*Proof.* For convenience, when considering points in  $\mathcal{P}_N$ , we always choose their unique preimage in  $\mathbb{R}^n$  whose first coordinate is 0. Then, we may denote each point in  $\mathcal{P}_N$  by an  $(n-1)$ -tuple in  $\mathbb{R}^{n-1}$ . Let  $T_1, T_2, \dots \in \mathbb{R}^{n-1}$  be a Cauchy sequence of points in  $\mathcal{P}_N$ . For  $1 \leq i \leq n-1$ , we claim that  $(T_k^i)_{k \geq 1}$  also form a Cauchy sequence in  $\mathbb{R}$ : For any  $\varepsilon > 0$ , there exists  $M$  such that for  $k_1, k_2 > M$ , we have  $d_{\text{tr}}(T_{k_1}, T_{k_2}) < \varepsilon$ . By Definition 16,  $d_{\text{tr}}(T_{k_1}, T_{k_2}) \geq |0 - 0 - T_{k_2}^i + T_{k_1}^i| = |T_{k_1}^i - T_{k_2}^i|$ . Thus, for  $k_1, k_2 > M$ , we have

$$|T_{k_1}^i - T_{k_2}^i| < \varepsilon.$$

Suppose now that the Cauchy sequence  $(T_k^i)_{k \geq 1}$  converges to  $T_0^i \in \mathbb{R}$ . It suffices to show that

- (i)  $T_0 = (T_0^1, T_0^2, \dots, T_0^{n-1})$  represents a point in  $\mathcal{P}_N$ ;
- (ii)  $\lim_{k \rightarrow \infty} d_{\text{tr}}(T_k, T_0) = 0$ .

To show (ii), we argue that since  $(T_k^i)_{k \geq 1}$  converges to  $T_0^i$  for all  $1 \leq i \leq n-1$ , then for any  $\varepsilon > 0$  there exists  $M$  such that for  $k > M$ , we have  $|T_k^i - T_0^i| < \frac{\varepsilon}{2}$  for all  $1 \leq i \leq n-1$ . Then by Definition 16,

$$\begin{aligned} d_{\text{tr}}(T_k, T_0) &= \max_{1 \leq i \leq n-1} (0, T_k^i - T_0^i) - \min_{1 \leq i \leq n-1} (0, T_k^i - T_0^i) \\ &< \frac{\varepsilon}{2} - \left(-\frac{\varepsilon}{2}\right) = \varepsilon. \end{aligned}$$

So  $\lim_{k \rightarrow \infty} d_{\text{tr}}(T_k - T_0) = 0$ .

To show (i), note that each coordinate of  $T_0$ , including the first, is the limit of the corresponding coordinates of  $(T_k)_{k \geq 1}$ . Suppose  $T_0 \notin \mathcal{P}_N$ , then there exists  $1 \leq i < j < k < l \leq N$  such that one term of  $T_0$  in (2) is strictly greater than the remaining two. Then there exists  $M_2$  such that for all  $k > M_2$ , the one term of  $T_k$  in (2) is also strictly greater than the remaining two, thus  $T_k \notin \mathcal{P}_N$ —a contradiction. Hence (i) holds, and  $\mathcal{P}_N$  is complete.  $\square$

**Proposition 34.**  $\mathcal{P}_N$  is separable.

*Proof.* We claim that the set of all trees with all rational coordinates is dense in  $\mathcal{P}_N$ : Fix any tree  $T = (w_{ij}) \in \mathcal{P}_N$ . By Proposition 27,  $T$  belongs to a polyhedron and there exists a tree topology with  $(N-3)$  internal edges. Then the distance between any two leaves is the sum of the lengths of the edges along the unique path connecting them. The number of edges along each path is at most  $(N-1)$ . For any  $\varepsilon > 0$  and length  $b_k$  of each edge of the tree  $T$ , since  $\mathbb{Q}$  is dense in  $\mathbb{R}$ , we can find a rational number  $q_k$  such that  $|q_k - b_k| < \frac{1}{2(N-1)}\varepsilon$ . Now, construct another tree  $T' = (w'_{ij})$  with the same topology as  $T$ , and with corresponding edge lengths  $q_k$ . Then for any  $1 \leq i < j \leq N$  we have that  $|w'_{ij} - w_{ij}| < \frac{\varepsilon}{2}$ . Thus

$$d_{\text{tr}}(T', T) = \max_{1 \leq i < j \leq n} (|w'_{ij} - w_{ij}|) - \min_{1 \leq i < j \leq n} (|w'_{ij} - w_{ij}|) < \varepsilon,$$

and all coordinates of  $q_k$  are rational. Thus,  $\mathcal{P}_N$  is separable.  $\square$

In addition, we have the following characterization of compact subsets in  $\mathbb{R}^n$ .

**Theorem 35** (Heine–Borel Theorem (Conway, 2014, Theorem 1.4.8)). *In the Euclidean space  $\mathbb{R}^n$ , a subset is compact if and only if it is closed and bounded.*

Thus, for palm tree space, there exist compact subsets in palm tree space.

**Corollary 36.** *In  $\mathcal{P}_N$ , a subset is compact if and only if it is closed and bounded.*

### 3.6 Probability Measures and Means in Palm Tree Space

We showed in Section 3.5 that palm tree space is a Polish space, and thus exhibits desirable properties for rigorous probability and statistics. Such properties ensure well-behaved measure-theoretic properties, and in particular, allow for classical probabilistic and statistical studies, such as convergence in various modes, as well as ensuring that stochastic processes are well defined. We now study the existence of probabilistic and statistical quantities for parametric data analysis, such as probability measures and Fréchet means and variances.

#### 3.6.1 Tropical Measures of Central Tendency

For distributions in general metric spaces, there are various measures of central tendency. These may be framed in palm tree space as follows (and may be generalized by replacing the tropical metric  $d_{\text{tr}}$  with any well-defined metric).

**Definition 37.** Given a probability space  $(\mathcal{T}_N, \mathcal{B}(\mathcal{T}_N), \mathbb{P}_{\mathcal{T}_N})$ , the quantity

$$\text{Var}_{\mathbb{P}_{\mathcal{T}_N}}(y) = \int_{\mathcal{T}_N} d_{\text{tr}}(y, x)^2 d\nu(x) < \infty \quad (5)$$

is known as the *tropical Fréchet variance*. The minimizer of the quantity (5) is the *tropical Fréchet population mean* or *barycenter*  $\mu_F$  of a distribution  $\nu$ :

$$\mu_{\text{tr}}^F = \arg \min_y \int_{\mathcal{T}_N} d_{\text{tr}}(y, x)^2 d\nu(x) < \infty. \quad (6)$$

**Definition 38.** The *tropical Fermat–Weber point* of a distribution is a similarly-defined measure of central tendency, and can be thought of as a generalized median of a distribution in a general metric space:

$$\mu_{\text{tr}}^{FW} = \arg \min_y \int_{\mathcal{T}_N} d_{\text{tr}}(y, x) d\nu(x). \quad (7)$$

For general metric spaces, neither existence nor uniqueness of (6) nor (7) are guaranteed. Ohta (2012) proves a condition under which barycenters are guaranteed to exist.

**Lemma 39.** (Ohta, 2012, Lemma 3.2) *If  $(M, d)$  is a proper metric space, then any distribution  $\nu$  where  $\int_M d(y, x)^2 d\nu(x) < \infty$  has a barycenter.*

As a consequence of the Heine–Borel theorem (see Corollary 36), palm tree space is a proper metric space. Thus, (6) evaluated according to the tropical metric is guaranteed to exist. However, since geodesics are not unique in palm tree space, Fermat–Weber points and Fréchet means will also, in general, not be unique. It is known that the set of tropical Fermat–Weber points is a classical convex polytope; Lin and Yoshida (2018) present a formal and complete treatment of the Fermat–Weber point under the tropical metric.

Understanding properties of a Fréchet mean for sets of phylogenetic trees is an important question that has been a topic of recent active research. Algorithms to compute the Fréchet mean have been proposed in the BHV setting (Skwerer et al., 2018); properties of the Fréchet mean in the extrinsic case where the mean lies outside of tree space have been recently studied (Anaya et al., 2019), and in the case where it is computed by Sturm’s algorithm (Sturm, 2003), the convergence behavior remains unknown.

### 3.6.2 Tropical Probability Measures

Probability measures on combinatorial and phylogenetic trees have been previously discussed, for example by Aldous (1996) and Billera et al. (2001). This section is dedicated to an analogous discussion on palm tree space. In  $\mathcal{P}_N$ , the Borel  $\sigma$ -algebra  $\mathcal{B}(\mathcal{T}_N)$  is the  $\sigma$ -algebra generated by the open tropical balls  $B_{\text{tr}}$  of  $\mathcal{T}_N$ , given in Definition 28. We begin by providing the existence of probability measures on  $\mathcal{P}_N$ .

**Definition 40.** A *finite tropical Borel measure* on  $\mathcal{T}_N$  is a map  $\mu : \mathcal{B}(\mathcal{T}_N) \rightarrow [0, \infty)$  such that  $\mu(\emptyset) = 0$ , and for mutually disjoint Borel sets  $A_1, A_2, \dots \in \mathcal{B}(\mathcal{T}_N)$  implies that  $\mu(\bigcup_{i=1}^{\infty} A_i) = \sum_{i=1}^{\infty} \mu(A_i)$ . If in addition  $\mu(\mathcal{T}_N) = 1$ , then  $\mu$  is a *tropical Borel probability measure* on  $\mathcal{T}_N$ .

Since  $\mathcal{T}_N$  is a finite union of polyhedra in  $\mathbb{R}^n/\mathbb{R}\mathbf{1}$  (see Proposition 27), tropical Borel probability measures exist if finite tropical Borel measures  $\mu$  exist on  $\mathcal{T}_N$  by an appropriate scaling of the value of  $\mu$  on each polyhedron.

Alternatively, the existence of probability measures on  $\mathcal{T}_N$  can be seen by considering an arbitrary probability space  $(\Omega, \mathcal{F}, \mathbb{P})$  together with a measurable map  $X : \Omega \rightarrow \mathcal{T}_N$ . Such maps exist, since we have shown in Section 3 that  $\mathcal{T}_N$  is a Polish space and thus  $(\mathcal{T}_N, \mathcal{B}(\mathcal{T}_N))$  is a standard measurable space (e.g., Taylor (2012)). The probability space  $(\Omega, \mathcal{F}, \mathbb{P})$  is a measure space by assumption, thus also measurable. In this case, the map  $X$  is a random variable taking values in  $\mathcal{T}_N$ . Then,  $X$  induces a probability measure  $\mathbb{P}_{\mathcal{T}_N}$  on  $(\mathcal{T}_N, \mathcal{B}(\mathcal{T}_N))$  by the pushforward measure  $X_*\mathbb{P}$  of  $\mathbb{P}$  under  $X$ , known as the *distribution*, for all Borel sets  $A \in \mathcal{B}(\mathcal{T}_N)$ :

$$X_*\mathbb{P}(A) := \mathbb{P}(X^{-1}(A)) = \mathbb{P}(\{\omega \in \Omega \mid X(\omega) \in A\}).$$

*Example 41.* If  $\mathbb{P}_{\vartheta}$  is a probability measure parameterized by  $\vartheta$ , then we may obtain parametric probability distributions on  $(\mathcal{T}_N, \mathcal{B}(\mathcal{T}_N))$  induced by  $\mathbb{P}_{\vartheta}$ . In the Bayesian setting, if the measure  $\lambda$  gives the prior distribution of  $\vartheta$ , then the joint probability measure  $\mathbb{P}(\mathcal{T}_N, \vartheta)$  is given by the product measure  $\mathbb{P}_{\mathcal{T}_N} \times \lambda$ . Similarly, the conditional measure  $\mathbb{P}(\vartheta \mid \mathcal{T}_N)$  is also proportional to this same product measure, which can be seen by Bayes' rule, where for events  $B_1, B_2, \dots$  that partition the sample space, then for any event  $A$ ,

$$P(B_i \mid A) = \frac{P(A \mid B_i)P(B_i)}{P(A)}.$$

Additionally, for continuous random variables  $Y$  and  $Z$ , the conditional density  $f_{Z|Y}(z \mid y)$  satisfies

$$f_{Z|Y}(z \mid y) = \frac{f_{Y|Z}(y \mid z)f_Z(z)}{f_Y(y)}.$$

Specific probability measures analogous to classical probability distributions exist on  $\mathcal{P}_N$ , which we now exemplify. We note that these measures may be generalized to arbitrary compact subspaces of  $\mathcal{T}_N$  by Corollary 36.

By Proposition 27, since  $\mathcal{T}_N$  is a finite union of polyhedra in  $\mathbb{R}^n/\mathbb{R}\mathbf{1}$ , the *base measure* on palm tree space can be defined by assigning a probability of  $1/(2N - 5)!!$  to each polyhedron, and a uniform distribution within each polyhedron. Since each polyhedron is unbounded, the uniform distribution here would be an improper prior. A proper uniform distribution may be obtained by a rescaling of each polyhedron to be unitary.

An exponential family-type analog for palm tree space may be defined using the tropical metric as follows:

$$f(w) = C \cdot \exp\{d_{\text{tr}}(w, \mu_{\text{tr}}^0)\}, \quad (8)$$

where  $C$  is a normalizing constant, and  $\mu_0$  is taken to be a measure of central tendency, as discussed above in Section 3.6.1. Measures of the form (8) give rise to families of distributions concentrated on a tropical central tree,  $\mu_{\text{tr}}^0$ .

## 4 Application to Data: Seasonal Influenza

We now provide an example of a statistical study in palm tree space following Yoshida et al. (2019). We demonstrate and compare statistical studies of tropical versus BHV principal component analysis (PCA) of the seasonal influenza virus by studying its diversity over twenty years of collected longitudinal data.

Influenza is an RNA virus affecting up to 10% of adults and 30% of children worldwide and on an annual basis, resulting in more than half a million deaths (WHO, 2016). Because of the rapid evolution of the virus genome, the development of an effective vaccine critically relies on being able to effectively visualize, analyze, and predict the viral evolution patterns in a statistically rigorous setting.

## 4.1 Influenza Data

We focus on the influenza type A virus, which is an RNA virus that is classified by subtype according to the two proteins occurring on the surface of the virus: hemagglutinin (HA) and neuraminidase (NA). Here, we focus on HA, which tends to be the most variable protein in genomic evolution, in terms of changing the antigenic make-up of surface proteins. Such antigenic variability (known as *antigenic drift*) is an important driving factor behind vaccine failure. We restrict our study to the subtype H3N2, which is becoming increasingly abundant, and a dominant factor studied in developing flu vaccines due to its recently increasing resistance to standard antiviral drugs (Altman, 2006). It was also the cause of an epidemic due to vaccine failure in 2002-2003 (CDC, 2004).

Genomic data for 1089 full length sequences of hemagglutinin (HA) for influenza A H3N2 from 1993 to 2017 in the state of New York were obtained from the GI-SAID EpiFlu™ database ([www.gisaid.org](http://www.gisaid.org)) and aligned with MUSCLE (Edgar, 2004) using default settings. HA sequences from each season were related to those of the preceding season. We then applied *tree dimensionality reduction* (Zairis et al., 2016) using temporal windows of 5 consecutive seasons to create 21 datasets. The date of each dataset corresponds to the first season; for example, the dataset dated 2013 consists of 5-leaved trees where the leaves come from seasons 2013 through 2017. Each unrooted tree in these datasets was constructed using the neighbor-joining method (Saitou and Nei, 1987) with Hamming distance. Outliers were then removed from each season using KDETREES (Scharndl et al., 2014). On average, there were approximately 20,000 remaining trees in each dataset. Finally, PCA was performed under the tropical metric (Yoshida et al., 2019) and under the BHV metric (Nye et al., 2017).

### 4.1.1 Tree Dimensionality Reduction

The influenza virus is assumed to emerge and evolve from a common ancestor: although the virus mutates each season and within each patient, each of these seasonal and patient-specific mutations can be traced back to a single virus (e.g., Liu et al. (2009)). This evolutionary pattern is depicted in a large phylogenetic tree. Tree dimensionality reduction is a sampling method that generates a data set of smaller trees via a structural and systematic sampling of the larger tree (Zairis et al., 2016). In other words, the method produces a collection of smaller trees that faithfully represents the evolutionary behavior of the single large tree, and thus allows the evolutionary information to be treated as a dataset with multiple points akin to bootstrapping, rather than viewing the large tree as a single datum. Specifically, this is done by randomly sampling one individual from each season over the length of the desired temporal window; each individual then gives one leaf of the reduced tree.

In the applications presented in Zairis et al. (2016), smaller trees were constructed with three, four, and five leaves; we follow within this size scale for consistency of the original method, but choose the largest number of leaves, since the two tree PCA methods were implemented in Nye et al. (2017) and Yoshida et al. (2019) for trees with a larger number of leaves.

## 4.2 PCA in Tree Spaces

PCA is a fundamental technique in descriptive and exploratory statistics that visualizes relationships within the data by reducing their dimensionality. As such, PCA has many important implications—for example, it projects to the subspace of the solution of  $k$ -means clustering (Ding and He, 2004)—and may be interpreted in several different ways. One interpretation may be seen as searching for a lower-dimensional plane that minimizes the sum of squared distances from the data points to the plane, and then finding an orthogonal projection from the data points onto the plane to visualize them. More precisely, given a set  $X$  of data points  $\{x_1, x_2, \dots, x_n\}$  where each  $x_i \in \mathbb{R}^m$ ,  $i = 1, \dots, n$ , we may consider a subset of  $k + 1$  of these points

$V = \{v_0, \dots, v_k\} \subset \mathbb{R}^m$  and define

$$\Pi(V) := \left\{ \sum_{i=0}^k p_i v_i \mid p_0, \dots, p_k \in \mathbb{R} \text{ such that } p_0 + \dots + p_k = 1 \right\},$$

where  $\Pi(V)$  is the affine subspace of  $\mathbb{R}^m$  containing  $V$ . The orthogonal  $L^2$  distance between any point  $y \in \mathbb{R}^m$  and  $\Pi(V)$  is denoted by  $d(y, \Pi(V))$ ; the squared of projected distances for the data  $X$  onto  $\Pi(V)$  is then

$$D_X^2(\Pi(V)) = \sum_{i=1}^n d(x_i, \Pi(V))^2.$$

The  $k$ th principal component  $\Pi_k$  is the choice of  $V$  minimizing  $D_X^2$ . In Euclidean space,  $\Pi_0$  corresponds to the sample mean, while  $\Pi_1$  is the regression line passing through the mean, and so on, for higher dimensions. These principal components are nested:  $\Pi_0 \subset \Pi_1 \subset \Pi_2 \subset \dots$ . This interpretation relies heavily on the setting of a vector space, since  $\Pi(V)$  is a linear combination of vectors, and visualizing the data on  $\Pi(V)$  relies on orthogonal projection, both of which are inherently linear algebraic notions, and hence difficult to directly implement in tree spaces.

It is important to emphasize that PCA is a descriptive and exploratory technique for data, and a form of unsupervised learning. As such, there is no *a priori* assumption on the distribution of the data, despite the coincidence of the above mentioned description of the technique with classical linear regression, which is an inferential tool (and thus, classically, assumes some distributional properties). PCA can always be used to reduce the dimensionality of and visualize data, no matter what their distribution (and no matter what interpretation of PCA is adapted to implement the procedure).

Respective adaptations of the above-mentioned interpretation of PCA to palm tree space and BHV space are given by Nye et al. (2017) and Yoshida et al. (2019): convex, triangular regions—the tropical triangle and the *locus* of weighted Fréchet means computed with respect to the BHV metric, respectively—define notions of second principal components in the respective spaces. Following Nye (2014), in the setting of phylogenetic tree space, we seek a convex hull of  $k + 1$  points to represent the  $k$ th principal component,  $\Pi(V)$  where now each  $v_i$  in  $V = \{v_0, \dots, v_k\}$  is a tree. Since any geodesic segment is the convex hull of its endpoints, a natural extension to the plane, or second principal component, would be to use the convex hull of three points. This also gives us a representation with projections that are readily visualizable.

In other words, we seek a 2-plane defined by three ultrametric trees and visualize the data by restricting and projecting onto the convex hull of these three points. In palm tree space, this is straightforward since tropical triangles are always 2-dimensional (Lin et al., 2017). In BHV space, however, this entails finding a locus, which is constructed from the set of discrete Fréchet means weighted by values on the probability simplex. As opposed to BHV triangles, the dimensionality of loci of weighted Fréchet means computed under the BHV metric is well behaved (Nye et al., 2017).

#### 4.2.1 Tropical PCA

The (tropically-) convex hull we seek in palm tree space by implementing the method of Yoshida et al. (2019) represents the second principal component is the tropical triangle. Edges are given by tropical line segments between their three vertices. Projections of data points onto the tropical triangle are exact and unique.

To build the tropical triangles, we seek three points within the dataset; in this sense, the PCA method is approximate and not exact. For smaller datasets, such a search may be combinatorially tractable. For larger datasets, we implement a Markov chain Monte Carlo (MCMC) algorithm to find these three points (Kang and Yoshida, 2018). Briefly, the idea is to first choose three points from the dataset at random and calculate the sums of the tropical distances of the remaining points to the tropical triangle initially defined by the three points. One point among these vertices is then randomly chosen to be iteratively replaced by other points within the dataset to find a smaller sum of tropical distances to the resulting triangles until a minimal sum of tropical distances is found; the corresponding three vertices of the triangle are then retained to define the second tropical principal components. Unlike in classical Euclidean PCA where the components are mutually orthogonal, the vertices of the tropical triangle onto which the data points are projected are in general not. The projections of the data points onto the tropical triangle are tropically-convex combinations

of the vertices. This procedure was run 5 times on each of the 21 datasets; each iteration was run in parallel on 18 CPU cores—Intel(R) Xeon(R) W-2155 CPU @ 3.30 GHz—and took approximately two hours to terminate, for a total of around 210 CPU hours to complete the tropical PCA procedure.

#### 4.2.2 BHV PCA

Since geodesic triangles (and more generally, polytopes) in BHV space are not well-behaved convex hulls (see Corollary 13), they are thus problematic candidates for BHV second principal components. An alternative method proposed by Nye et al. (2017) searches for the *locus* of weighted, discrete, Fréchet means computed with respect to the BHV metric as a BHV  $k$ th principal component.

Briefly, for the weighted, discrete, BHV Fréchet mean,

$$\mu(V, w) = \arg \min_{y \in \mathcal{T}_N^{\text{BHV}}} \sum_{i=0}^k w_i \cdot d_{\text{BHV}}(y, v_i)^2,$$

if the weights are given by elements in the  $k$ -dimensional simplex of probability vectors,

$$\mathcal{S}^k := \left\{ (p_0, \dots, p_k) \mid p_i \geq 0, i = 0, \dots, k, \sum_{i=0}^k p_i = 1 \right\},$$

then  $\Pi(V)$  defined by

$$\Pi(V) := \{ \mu(V, p) \mid p \in \mathcal{S}^k \}$$

is the locus of the Fréchet mean of  $V$ . Geometric properties of the locus, such as convexity and dimensionality, are well-behaved, as opposed to BHV convex hulls. In our application, we implement the algorithm by Bačák to compute the weighted, discrete, BHV Fréchet means and thus construct the locus (Bačák, 2014). Projections of data points onto the locus are approximate and need not be unique.

Similar to the tropical PCA case described above, the procedure is approximate and uses trees from the dataset to construct the locus and its boundaries. We follow the algorithm proposed in the original reference, which is also a stochastic optimization algorithm. As in the tropical PCA case, the procedure was run 5 times on each of the 21 datasets; each iteration was run in parallel on 18 CPU cores—Intel(R) Xeon(R) W-2155 CPU @ 3.30 GHz—and also took approximately two hours to terminate, for a total of also around 210 CPU hours to complete the BHV PCA procedure.

#### Software and Data Availability

Software to compute both tropical and BHV PCA is publicly available in R and Java code. Their implementation to the influenza data described in this paper is located on the FluPCA GitHub repository at <https://github.com/antheamonod/FluPCA>.

The data used in this paper were obtained from publicly available sources and preprocessed, as detailed in Section 4.1. The final version used in the analyses in this paper are also publicly available on the FluPCA GitHub repository.

The resulting figures from both BHV and tropical PCA projections for all 21 data sets are also available on the FluPCA GitHub repository.

### 4.3 Interpretation of Tree PCA

In the tropical case, the second principal component represented by the tropical triangle—whose vertices are given by three ultrametric trees, and whose edges are given by the tropical line segments between them—divides into cells, which are determined by the tree topologies that an edge (tropical line segment) traverses. Trees in the dataset are then projected into the cells corresponding to their topologies in the PCA visualization. The simplest case in both tropical PCA is where all three vertices of the triangle are of the same tree topology, then there will only be one cell and all projections will be of the same topology; if two points are trees of the same tree topology, then every point on the tropical line segment connecting

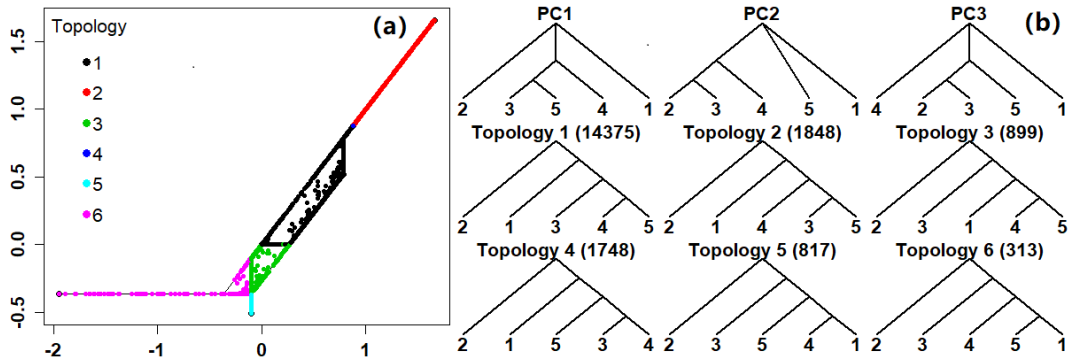


Figure 4: 2008: The tropical triangle as the second tropical principal component. (a) Tropical triangle and projected data points; (b) Vertices of the tropical triangle and projected tree topologies.

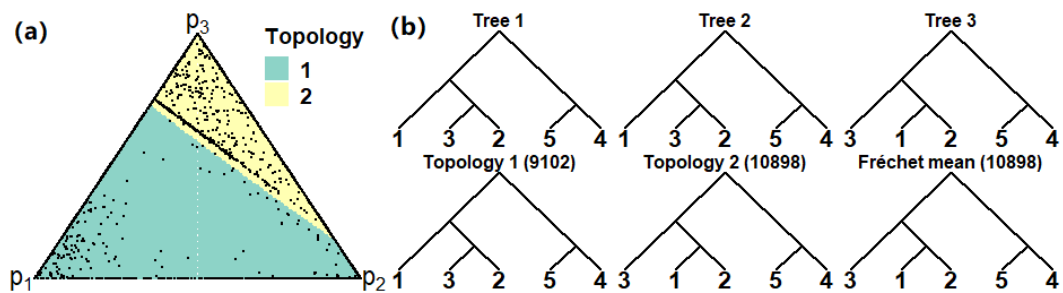


Figure 5: 2008: The locus of BHV Fréchet means as the second principal component. (a) The simplex shaded by topology of corresponding points on the affine subspace; (b) Trees 1, 2, and 3 correspond to three weighted Fréchet means.

them will also be of the same tree topology. An example can be seen in the 1993 data set, available at <https://github.com/antheamonod/FluPCA/Figures>.

A more interesting example can be seen in the 2008 dataset in Figure 4. The tropical triangle divides into six cells; a complete discussion on tropical polytopes, their decomposition into cells and their self-duality can be found in Section 5.2 of Maclagan and Sturmfels (2015), Theorem 5.2.21 in particular gives the isomorphism from a tropical polytope to its self-dual. As conjectured in Yoshida et al. (2019), one possible biological interpretation of the cells is that neighboring cells represent similar yet distinct tree structures differing by tree rearrangements of one move. Tree rearrangements are used in algorithms where the goal is to search for the optimal tree structure in statistical tree reconstruction methods (see e.g., Bordewich and Semple (2005); Felsenstein (2004)). The tropical line segment forming the topmost edge of the triangle traverses five different tree topologies (indicated by the pink, green, black, blue, and red points along the topmost line segment), indicating that the three vertices of the triangle are quite different from one another in terms of tree topology.

The BHV locus, which represents the second principal component in BHV space, is also generated by three vertices (ultrametric trees), and depicted in the BHV PCA plots by a triangle. Here, varying tree topologies are depicted by the multicolored patches within the triangular region, indicating that the locus straddles several orthants in BHV space. In the 2008 dataset in Figure 5, the locus straddles two BHV orthants and we see two tree topologies occurring among the projected points.

In the 2008 dataset, palm tree space and the tropical geometric approach to computations in phylogenetic tree space appears to allow for occurrences of richer and more subtle structures and methods: in these examples, we see tropical PCA projections of six different topologies, versus two in the BHV case.

Table 1: Proportion of Explained Variance for Tropical and BHV PCA

	1993	1994	1995	1996	1997	1998	1999
Tropical	0.7269	0.8505	<b>0.9577</b>	0.7482	0.8437	0.8790	0.8564
BHV	0.3019	0.4347	0.3151	0.5025	0.0505	0.6408	<b>0.9524</b>
	2000	2001	2002	2003	2004	2005	2006
Tropical	0.7942	0.8302	0.9525	0.8622	0.7931	0.8304	0.7300
BHV	<b>0.0014</b>	0.9488	0.8962	0.4927	0.3651	0.3634	0.2383
	2007	2008	2009	2010	2011	2012	2013
Tropical	0.6995	<b>0.4637</b>	0.6289	0.6665	0.5920	0.5568	0.5624
BHV	0.2727	0.0460	0.1563	0.1935	0.2771	0.1998	0.1279

#### 4.4 Results: Proportion of Explained Variance $R^2$

In terms of explained variance given in Table 1, we see that in general, tropical PCA is able to explain more of the variance in the data than does BHV PCA. BHV PCA results also have a higher variability over a wider range than tropical PCA: BHV PCA explains between  $\sim 0.0\%$  and  $95\%$  of the variance, while tropical PCA explains between  $46\%$  and  $96\%$ .

## 5 Discussion

In this paper, we defined palm tree space as the space of phylogenetic trees with  $N$  leaves, endowed with the tropical metric. We gave results on its analytic, topological, geometric, and combinatorial properties and showed that they are conducive to rigorous treatments and studies in probability, and demonstrated that descriptive statistical analysis on real data is also feasible. We showed that in certain respects, certain properties of palm tree space are more natural and amenable to statistical analyses than BHV space. An important difference, however, is that geodesics in palm tree space are not unique. Our work invites the reinterpretation of existing statistical methods in terms of the tropical metric to make a wider array of exact analyses readily available and interpretable to phylogenetic research with potential impact for biological discoveries.

### Biological and Statistical Implications

Despite the statistical challenges of arbitrariness of dimension of BHV polytopes and stickiness described in Section 3.1, the BHV parameterization has been successfully implemented to reveal important biological findings (e.g., Zairis et al. (2014)). In terms of interpretation, the unresolved singularities of BHV Fréchet means translate to “indecisiveness” of which branching patterns or tree topologies are “preferred,” which is consistent with what is often seen in some biological settings where the trees arise from sequence alignment. However, mathematically, trees are used to model other biological phenomena, such as pulmonary paths as airway trees (e.g., Feragen et al. (2013, 2015)); brain growth and structure (e.g., Yan and Yan (2013)); and neuronal morphologies (e.g., Kanari et al. (2018)). Such a probabilistic assumption may not be reasonable in these other settings. Given recent research interest in developing methods to bypass these difficulties support the goal of our work, which is that alternative representations is an important direction (e.g., Anaya et al. (2019); Skwerer et al. (2018)). An important and interesting direction for future research is the identification of non-uniform probability distributions in the tropical setting, which is challenging yet promising: Tran (2018) outlines various ways in which tropical Gaussian distributions may be constructed.

In the context of shape statistics (Kendall, 1989) and computational anatomy (Grenander and Miller, 1998), the data objects of interest are often modeled as elements of algebraic spaces. In particular, these algebraic spaces are quotient spaces generated by group actions. Recent work has studied the behavior of estimators on such spaces, uncovering undesirable properties, such as biasedness and inconsistency when the group actions are random (that is, when the quotient spaces are generated by elements of the group are chosen at random to act on the topological space) or continuous (as in the case of Lie groups acting on Riemannian manifolds) (Devilliers et al., 2017; Miolane and Pennec, 2015). Nonparametric methods

have been developed to bypass the problem of inconsistency by Bhattacharya and Patrangenaru (2014). As previously mentioned in Section 2.2.3, the tropical projective torus  $\mathbb{R}^n/\mathbb{R}\mathbf{1}$  is a quotient space that may be generated by a group action, however the biasedness and inconsistency in previous work arise due to the poor behavior of the transformed metric after it is mapped into the quotient space, which results in a pseudometric. In our case, the tropical metric is well-behaved and defined directly on the quotient space, therefore differing in setting to previous work.

It should also be noted (as discussed in Section 3.3.1) that the non-uniqueness property of geodesics in palm tree space poses computational difficulties, but does not prohibit statistical analysis and can still yield useful descriptive as well as inferential information, for example, on clustering behavior. Another important setting where geodesics are not unique is that of positively-curved spaces. Bhattacharya and Bhattacharya (2008) study asymptotic behavior and distributions on Riemannian manifolds, including positively curved manifolds. Recent work such as that by Kobayashi and Wynn (2019) develops techniques for data analysis on curved spaces by tuning the geodesic metrics accordingly. In particular, a general Fréchet function is defined, and its parameters are chosen accordingly, depending on the goal: for example, one geodesic metric may be transformed into another to control the curvature of the space for data analysis. There are large bodies of existing work in related areas on curved spaces, for example, in the case of manifold learning; shape statistics; Wasserstein spaces for probability measures; and information geometry. Though these domains each have their own specific goals and studies, data analysis and computation play a central role in these settings. Moreover, there are known settings in these related areas where positive curvature, and thus non-uniqueness of geodesics, arises (for example, the 2-Wasserstein space for Gaussian measures is positively curved (Takatsu, 2011)). Adapting existing techniques in these settings to statistical analysis in palm tree space is an important direction of research that merits exploration.

## Acknowledgments

The authors are grateful to Robert J. Adler, Omer Bobrowski, Ioan Filip, Maia Fraser, Stephan Huckemann, Elliot Paquette, Juan Ángel Patiño-Galindo, Yitzchak (Elchanan) Solomon, and Bernd Sturmfels for helpful discussions. We are especially indebted to Carlos Améndola and Hossein Khiabani for their extensive commentary, suggestions, and support throughout the course of this project.

A.M. and R.Y. wish to acknowledge the Mathematisches Forschungsinstitut Oberwolfach (MFO) for hosting their visit in January 2018, which inspired this work. B.L. wishes to acknowledge support by the Simons Foundation and the hospitality of the Institut Mittag-Leffler during the spring of 2018, where a large part of this research was carried out.

The authors would also like to acknowledge the GI-SAID EpiFlu™ initiative for making the data used in this study publicly available.

R.Y. is supported in part by NSF DMS #1622369 and #1916037. Any opinions, findings, and conclusions or recommendations expressed in this material are those of the author(s) and do not necessarily reflect the views of any of the funders.

## Author Contributions Statement

A.M. conceived the study and designed the research. A.M., B.L., and R.Y. performed research. A.M. and R.Y. developed the algorithms; Q.K. implemented the software and performed the analyses. A.M. wrote the manuscript.

## Competing Financial Interests Statement

The authors declare that no competing financial interests exist.

## References

- Akian, M., S. Gaubert, V. Nițică, and I. Singer (2011). Best Approximation in Max-plus Semimodules. *Linear Algebra and its Applications* 435(12), 3261–3296.
- Aldous, D. (1996). Probability Distributions on Cladograms. In D. Aldous and R. Pemantle (Eds.), *Random Discrete Structures*, New York, NY, pp. 1–18. Springer New York.
- Allen, B. L. and M. Steel (2001). Subtree Transfer Operations and Their Induced Metrics on Evolutionary Trees. *Annals of Combinatorics* 5(1), 1–15.
- Allman, E. S. and J. A. Rhodes (2008). Phylogenetic ideals and varieties for the general Markov model. *Advances in Applied Mathematics* 40(2), 127–148.
- Altman, L. K. (2006). This Season’s Flu Virus Is Resistant to 2 Standard Drugs. <https://www.nytimes.com/2006/01/15/health/this-seasons-flu-virus-is-resistant-to-2-standard-drugs.html>.
- Améndola, C., M. Casanellas, and L. D. G. Puente (2018). Tapas of Algebraic Statistics. *Notices of the AMS* 65(8).
- Anaya, M., O. Anipchenko-Ulaj, A. Ashfaq, J. Chiu, M. Kaiser, M. S. Ohsawa, M. Owen, E. Pavlechko, K. St. John, S. Suleria, K. Thompson, and C. Yap (2019). Properties for the Fréchet Mean in Billera–Holmes–Vogtmann Treespace. *arXiv:1907.05937*.
- Ardila, F. and C. J. Klivans (2006). The Bergman Complex of a Matroid and Phylogenetic Trees. *Journal of Combinatorial Theory, Series B* 96(1), 38–49.
- Baez, J. C. and N. Otter (2017). Operads and phylogenetic trees. *Theory and Applications of Categories* 32(40), 1397–1453.
- Barden, D. and H. Le (2018). The logarithm map, its limits and Fréchet means in orthant spaces. *Proceedings of the London Mathematical Society* 117(4), 751–789.
- Barden, D., H. Le, M. Owen, et al. (2013). Central limit theorems for fréchet means in the space of phylogenetic trees. *Electronic journal of probability* 18.
- Bačák, M. (2014). Computing Medians and Means in Hadamard Spaces. *SIAM Journal on Optimization* 24(3), 1542–1566.
- Benner, P., M. Bačák, and P.-Y. Bourguignon (2014). Point Estimates in Phylogenetic Reconstructions. *Bioinformatics* 30(17), i534–i540.
- Bhattacharya, A. and R. Bhattacharya (2008). Statistics on Riemannian Manifolds: Asymptotic Distribution and Curvature. *Proceedings of the American Mathematical Society* 136(8), 2959–2967.
- Bhattacharya, R. and V. Patrangenaru (2014). Statistics on manifolds and landmarks based image analysis: A nonparametric theory with applications. *Journal of Statistical Planning and Inference* 145, 1–22.
- Billera, L. J., S. P. Holmes, and K. Vogtmann (2001). Geometry of the Space of Phylogenetic Trees. *Advances in Applied Mathematics* 27(4), 733–767.
- Bordewich, M. and C. Semple (2005, Jan). On the Computational Complexity of the Rooted Subtree Prune and Regraft Distance. *Annals of Combinatorics* 8(4), 409–423.
- Bourbaki, N. (2004). *Elements of Mathematics: Integration I*.
- Buneman, P. (1974). A Note on the Metric Properties of Trees. *Journal of Combinatorial Theory, Series B* 17(1), 48–50.
- Butkovič, P. (2010). *Max-Linear Systems: Theory and Algorithms*. Springer Monographs in Mathematics. London: Springer–Verlag.

- Cardona, G., A. Mir, F. Rosselló, L. Rotger, and D. Sánchez (2013). Cophenetic Metrics for Phylogenetic Trees, After Sokal and Rohlf. *BMC Bioinformatics* 14(1), 3.
- Cauchy, A.-L. (1821). Sur les formules qui résultent de l'emploi du signe et sur  $>$  ou  $<$ , et sur les moyennes entre plusieurs quantités. *Cours d'Analyse, 1er Partie: Analyse algébrique*, 373–377.
- CDC (2004). Preliminary assessment of the effectiveness of the 2003-04 inactivated influenza vaccine—Colorado, December 2003. *MMWR. Morbidity and mortality weekly report* 53(1), 8.
- Cohen, G., S. Gaubert, and J.-P. Quadrat (2004). Duality and Separation Theorems in Idempotent Semi-modules. *Linear Algebra and its Applications* 379, 395–422. Special Issue on the Tenth ILAS Conference (Auburn, 2002).
- Conway, J. B. (2014). *A Course in Point Set Topology*. Undergraduate Texts in Mathematics. Springer, Cham.
- Devadoss, S. L. and J. Morava (2015). Navigation in Tree Spaces. *Advances in Applied Mathematics* 67, 75–95.
- Devilliers, L., S. Allasonnière, A. Trouvé, and X. Pennec (2017). Template Estimation in Computational Anatomy: Fréchet Means Top and Quotient Spaces Are Not Consistent. *SIAM Journal on Imaging Sciences* 10(3), 1139–1169.
- Ding, C. and X. He (2004). K-means clustering via principal component analysis. In *Proceedings of the Twenty-First International Conference on Machine Learning*, pp. 29. ACM.
- Edgar, R. C. (2004, 03). MUSCLE: Multiple sequence alignment with high accuracy and high throughput. *Nucleic Acids Research* 32(5), 1792–1797.
- Edwards, A. W. F. (1970). Estimation of the Branch Points of a Branching Diffusion Process. *Journal of the Royal Statistical Society. Series B (Methodological)* 32(2), 155–174.
- Einmahl, J. H. J., A. Kiriliouk, and J. Segers (2018, Jun). A continuous updating weighted least squares estimator of tail dependence in high dimensions. *Extremes* 21(2), 205–233.
- Evans, S. N. and F. A. Matsen (2012). The phylogenetic Kantorovich–Rubinstein metric for environmental sequence samples. *Journal of the Royal Statistical Society: Series B (Statistical Methodology)* 74(3), 569–592.
- Felsenstein, J. (1981). Evolutionary Trees from DNA Sequences: A Maximum Likelihood Approach. *Journal of Molecular Evolution* 17(6), 368–376.
- Felsenstein, J. (2004). *Inferring phylogenies*, Volume 2. Sinauer associates Sunderland, MA.
- Feragen, A., P. Lo, M. de Bruijne, M. Nielsen, and F. Lauze (2013, Aug). Toward a Theory of Statistical Tree-Shape Analysis. *IEEE Transactions on Pattern Analysis and Machine Intelligence* 35(8), 2008–2021.
- Feragen, A., M. Owen, J. Petersen, M. M. W. Wille, L. H. Thomsen, A. Dirksen, and M. de Bruijne (2013). Tree-Space Statistics and Approximations for Large-Scale Analysis of Anatomical Trees. In J. C. Gee, S. Joshi, K. M. Pohl, W. M. Wells, and L. Zöllei (Eds.), *Information Processing in Medical Imaging*, Berlin, Heidelberg, pp. 74–85. Springer Berlin Heidelberg.
- Feragen, A., J. Petersen, M. Owen, P. Lo, L. H. Thomsen, M. M. W. Wille, A. Dirksen, and M. de Bruijne (2015, June). Geodesic Atlas-Based Labeling of Anatomical Trees: Application and Evaluation on Airways Extracted From CT. *IEEE Transactions on Medical Imaging* 34(6), 1212–1226.
- Fitch, W. M. (1971). Toward Defining the Course of Evolution: Minimum Change for a Specific Tree Topology. *Systematic Biology* 20(4), 406–416.
- Fitch, W. M. and E. Margoliash (1967). Construction of Phylogenetic Trees. *Science* 155(3760), 279–284.

- Foulds, L. R. and R. L. Graham (1982). The Steiner Problem in Phylogeny is NP-Complete. *Advances in Applied Mathematics* 3(1), 43–49.
- Gavryushkin, A. and A. J. Drummond (2016). The Space of Ultrametric Phylogenetic Trees. *Journal of Theoretical Biology* 403, 197–208.
- Grenander, U. and M. I. Miller (1998). Computational anatomy: An emerging discipline. *Quarterly of applied mathematics* 56(4), 617–694.
- Holmes, S. (2003). Statistics for Phylogenetic Trees. *Theoretical Population Biology* 63(1), 17–32.
- Holmes, S. (2005). Statistical Approach to Tests Involving Phylogenies. *Mathematics of Evolution and Phylogeny*, 91–120.
- Hotz, T., S. Huckemann, H. Le, J. S. Marron, J. C. Mattingly, E. Miller, J. Nolen, M. Owen, V. Patrangenaru, and S. Skwerer (2013). Sticky Central Limit Theorems on Open Books. *The Annals of Applied Probability* 23(6), 2238–2258.
- Huckemann, S., J. Mattingly, E. Miller, and J. Nolen (2015). Sticky central limit theorems at isolated hyperbolic planar singularities. *Electron. J. Probab.* 20, 34 pp.
- Jardine, C., N. Jardine, and R. Sibson (1967). The Structure and Construction of Taxonomic Hierarchies. *Mathematical Biosciences* 1(2), 173–179.
- Juhl, D., D. M. Warme, P. Winter, and M. Zachariasen (2018). The GeoSteiner software package for computing Steiner trees in the plane: An updated computational study. *Mathematical Programming Computation* 10(4), 487–532.
- Kanari, L., P. Dłotko, M. Scolamiero, R. Levi, J. Shillcock, K. Hess, and H. Markram (2018, Jan). A Topological Representation of Branching Neuronal Morphologies. *Neuroinformatics* 16(1), 3–13.
- Kang, Q. and R. Yoshida (2018). Estimating Tropical Principal Components Using Metropolis Hastings Algorithm. In *International Congress on Mathematical Software*, pp. 272–279. Springer.
- Kendall, D. G. (1989). A Survey of the Statistical Theory of Shape. *Statistical Science* 4(2), 87–99.
- Kobayashi, K. and H. P. Wynn (2019, Feb). Empirical geodesic graphs and CAT(k) metrics for data analysis. *Statistics and Computing*.
- Lin, B., B. Sturmfels, X. Tang, and R. Yoshida (2017). Convexity in Tree Spaces. *SIAM Journal on Discrete Mathematics* 31(3), 2015–2038.
- Lin, B. and N. M. Tran (2019). Two-player incentive compatible outcome functions are affine maximizers. *Linear Algebra and its Applications* 578, 133–152.
- Lin, B. and R. Yoshida (2018). Tropical Fermat–Weber Points. *SIAM Journal on Discrete Mathematics*. To appear. Available at arXiv:1604.04674.
- Liu, S., K. Ji, J. Chen, D. Tai, W. Jiang, G. Hou, J. Chen, J. Li, and B. Huang (2009, 03). Panorama Phylogenetic Diversity and Distribution of Type A Influenza Virus. *PLOS ONE* 4(3), 1–20.
- Long, C. and S. Sullivant (2015). Identifiability of 3-class Jukes–Cantor mixtures. *Advances in Applied Mathematics* 64, 89–110.
- Maclagan, D. and B. Sturmfels (2015). *Introduction to Tropical Geometry (Graduate Studies in Mathematics)*. American Mathematical Society.
- Manon, C. (2011). Dissimilarity Maps on Trees and the Representation Theory of  $SL_m(\mathbb{C})$ . *Journal of Algebraic Combinatorics* 33(2), 199–213.
- Miller, E., M. Owen, and J. S. Provan (2015). Polyhedral computational geometry for averaging metric phylogenetic trees. *Advances in Applied Mathematics* 68, 51–91.

- Miolane, N. and X. Pennec (2015). Biased Estimators on Quotient Spaces. In F. Nielsen and F. Barbaresco (Eds.), *Geometric Science of Information*, Cham, pp. 130–139. Springer International Publishing.
- Munch, E. and A. Stefanou (2019). The  $\ell^\infty$ -Cophenetic Metric for Phylogenetic Trees as an Interleaving Distance. In *Research in Data Science*, pp. 109–127. Springer.
- Nye, T. M. W. (2011). Principal Components Analysis in the Space of Phylogenetic Trees. *The Annals of Statistics* 39(5), 2716–2739.
- Nye, T. M. W. (2014). An Algorithm for Constructing Principal Geodesics in Phylogenetic Treespace. *IEEE/ACM Trans. Comput. Biol. Bioinformatics* 11(2), 304–315.
- Nye, T. M. W., X. Tang, G. Weyenberg, and R. Yoshida (2017). Principal Component Analysis and the Locus of the Fréchet Mean in the Space of Phylogenetic Trees. *Biometrika* 104(4), 901–922.
- Ohta, S.-I. (2012). Barycenters in Alexandrov Spaces of Curvature Bounded Below. *Advances in Geometry* 14(4).
- Owen, M. and J. S. Provan (2011). A Fast Algorithm for Computing Geodesic Distances in Tree Space. *IEEE/ACM Trans. Comput. Biol. Bioinformatics* 8(1), 2–13.
- Pachter, L. and B. Sturmfels (2004). Tropical geometry of statistical models. *Proceedings of the National Academy of Sciences* 101(46), 16132–16137.
- Pachter, L. and B. Sturmfels (2005). *Algebraic Statistics for Computational Biology*, Volume 13. Cambridge University Press.
- Parthasarathy, K. (1967). Probability and Mathematical Statistics: A Series of Monographs and Textbooks. In *Probability Measures on Metric Spaces*, Probability and Mathematical Statistics: A Series of Monographs and Textbooks, pp. ii. Academic Press.
- Rannala, B. and Z. Yang (1996). Probability Distribution of Molecular Evolutionary Trees: A New Method of Phylogenetic Inference. *Journal of Molecular Evolution* 43(3), 304–311.
- Rhodes, J. A. and S. Sullivant (2012). Identifiability of large phylogenetic mixture models. *Bulletin of mathematical biology* 74(1), 212–231.
- Roch, S. and A. Sly (2017). Phase Transition in the Sample Complexity of Likelihood-Based Phylogeny Inference. *Probability Theory and Related Fields* 169(1), 3–62.
- Saitou, N. and M. Nei (1987). The Neighbor-Joining Method: A New Method for Reconstructing Phylogenetic Trees. *Molecular Biology and Evolution* 4(4), 406–425.
- Schardl, C. L., D. K. Howe, G. Weyenberg, P. M. Huggins, and R. Yoshida (2014, 04). KDETREES: Non-parametric estimation of phylogenetic tree distributions. *Bioinformatics* 30(16), 2280–2287.
- Schröder, E. (1870). Vier kombinatorische Probleme. *Z. Math. Phys* 15, 361–376.
- Schwarz, H. A. (1890). *Ueber ein die Flächen kleinsten Flächeninhalts betreffendes Problem der Variationsrechnung*, pp. 223–269. Berlin, Heidelberg: Springer Berlin Heidelberg.
- Skwerer, S., S. Provan, and J. Marron (2018). Relative Optimality Conditions and Algorithms for Treespace Fréchet Means. *SIAM Journal on Optimization* 28(2), 959–988.
- Sokal, R. R. and C. D. Michener (1958). A Statistical Method for Evaluating Systematic Relationships. *University of Kansas Science Bulletin* 38, 1409–1438.
- Sommerfeld, M. and A. Munk (2018). Inference for empirical Wasserstein distances on finite spaces. *Journal of the Royal Statistical Society: Series B (Statistical Methodology)* 80(1), 219–238.
- Speyer, D. and B. Sturmfels (2004). The Tropical Grassmannian. *Advances in Geometry* 4(3).

- Speyer, D. and B. Sturmfels (2009). Tropical mathematics. *Mathematics Magazine* 82(3), 163–173.
- St. John, K. (2016, 06). Review Paper: The Shape of Phylogenetic Treespace. *Systematic Biology* 66(1), e83–e94.
- Steel, M. A. and D. Penny (1993). Distributions of tree comparison metrics: Some new results. *Systematic biology* 42(2), 126–141.
- Steel, M. A. and L. A. Székely (2006, 08). On the variational distance of two trees. *Ann. Appl. Probab.* 16(3), 1563–1575.
- Sturm, K.-T. (2003). Probability measures on metric spaces of nonpositive curvature. *Heat Kernels and Analysis on Manifolds, Graphs, and Metric Spaces: Lecture Notes from a Quarter Program on Heat Kernels, Random Walks, and Analysis on Manifolds and Graphs: April 16-July 13, 2002, Emile Borel Centre of the Henri Poincaré Institute, Paris, France* 338, 357.
- Sturmfels, B. and S. Sullivant (2005). Toric ideals of phylogenetic invariants. *Journal of Computational Biology* 12(2), 204–228.
- Sullivant, S. (2018). *Algebraic Statistics*, Volume 194. American Mathematical Soc.
- Takatsu, A. (2011, 12). Wasserstein geometry of Gaussian measures. *Osaka J. Math.* 48(4), 1005–1026.
- Tavaré, S. (1986). Some probabilistic and statistical problems in the analysis of DNA sequences. *Lectures on mathematics in the life sciences* 17(2), 57–86.
- Taylor, J. C. (2012). *An Introduction to Measure and Probability*. Springer Science & Business Media.
- Tran, N. M. (2018). Tropical Gaussians: A Brief Survey. *arXiv preprint arXiv:1808.10843*.
- Waterman, M. S., T. F. Smith, and W. A. Beyer (1976). Some biological sequence metrics. *Advances in Mathematics* 20(3), 367–387.
- Weyenberg, G. and R. Yoshida (2016). Phylogenetic Tree Distances. In *Encyclopedia of Evolutionary Biology*, pp. 285–290. Elsevier.
- WHO (2016). World Health Organization — Influenza. <https://www.who.int/biologicals/vaccines/influenza/en/>.
- Willis, A. (2019). Confidence sets for phylogenetic trees. *Journal of the American Statistical Association* 114(525), 235–244.
- Willis, A. and R. Bell (2018). Uncertainty in phylogenetic tree estimates. *Journal of Computational and Graphical Statistics* 27(3), 542–552.
- Yan, B. C. and J. F. Yan (2013). A tree-like model for brain growth and structure. *J Biophys* 2013, 241612.
- Yoshida, R., L. Zhang, and X. Zhang (2019, Feb). Tropical Principal Component Analysis and Its Application to Phylogenetics. *Bulletin of Mathematical Biology* 81(2), 568–597.
- Zairis, S., H. Khiabani, A. J. Blumberg, and R. Rabadan (2014). Moduli spaces of phylogenetic trees describing tumor evolutionary patterns. In *International Conference on Brain Informatics and Health*, pp. 528–539. Springer.
- Zairis, S., H. Khiabani, A. J. Blumberg, and R. Rabadán (2016). Genomic Data Analysis in Tree Spaces. *arXiv:1607.07503*.